เสถียรภาพและการกักเก็บระดับนาโนเมตรของออกซีเรสเวอราทรอล

นายศรัณญู สอนกำเนิด

วิทยานิพนธ์นี้เป็นส่วนหนึ่งของการศึกษาตามหลักสูตรปริญญาวิทยาศาสตรมหาบัณฑิต
สาขาวิชาเคมี ภาควิชาเคมี
คณะวิทยาศาสตร์ จุฬาลงกรณ์มหาวิทยาลัย
ปีการศึกษา 2557

STABILITY AND NANO-ENCAPSULATION OF OXYRESVERATROL

Mr. Saranyoo Sornkamnird

A Thesis Submitted in Partial Fulfillment of the Requirements

for the Degree of Master of Science Program in Chemistry

Department of Chemistry

Faculty of Science

Chulalongkorn University

Academic Year 2014

Thesis Title	STABILITY AND NANO-ENCAPSULATION OF OXYRESVERATROL
By	Mr. Saranyoo Sornkamnird
Field of Study	Chemistry
Thesis Advisor	Assistant Professor Pattara Sawasdee, Ph.D.

Accepted by the Faculty of Science, Chulalongkorn University in Partial Fulfillment of the Requirements for the Master's Degree

.....Dean of the Faculty of Science
(Professor Supot Hannongbua, Dr.rer.nat.)

THESIS COMMITTEE

.....Chairman
(Associate Professor Vudhichai Parasuk, Ph.D.)

.....Thesis Advisor
(Assistant Professor Pattara Sawasdee, Ph.D.)

.....Examiner
(Associate Professor Supason Wanichwecharungruang, Ph.D.)

.....External Examiner
(Assistant Professor Panya Sunintaboon, Ph.D.)

ศรัณญู สอนกำเนิด : เสถียรภาพและการกักเก็บระดับนาโนเมตรของออกซีเรสเวอราทรอล (STABILITY AND NANO-ENCAPSULATION OF OXYRESVERATROL) อ.ที่ปรึกษาวิทยานิพนธ์หลัก: ผศ. ดร.พัฒทรา สวัสดี, 87 หน้า.

ทรานส์ออกซีเรสเวอราทรอล เป็นสารออกฤทธิ์ทางชีวภาพ ที่พบได้จากแก่นของต้นมะหาด ได้ถูกนำมาศึกษาความเสถียรต่อแสงและอุณหภูมิ โดยทำการศึกษาเปรียบเทียบกับทรานส์เรสเวอราทรอล ผลการศึกษาพบว่าทรานส์ออกซีเรสเวอราทรอลและทรานส์เรสเวอราทรอลมีความเสถียรต่อแสงฟลูออเรสเซนต์และอุณหภูมิเป็นระยะเวลา 7 วัน ในขณะที่รังสียูวีเอ เป็นสาเหตุที่ทำให้ทรานส์ออกซีเรสเวอราทรอลและทรานส์เรสเวอราทรอลเปลี่ยนโครงสร้างกลายเป็นซิส โดยทรานส์ออกซีเรสเวอราทรอลจะเกิดการเปลี่ยนแปลงได้เร็วกว่าทรานส์เรสเวอราทรอล ซิสออกซีเรสเวอราทรอลจะเปลี่ยนแปลงโครงสร้างกลับมาเป็นแบบทรานส์อีกครั้งเมื่อถูกกระตุ้นด้วยอุณหภูมิ ในขณะที่ซิสเรสเวอราทรอลสามารถเปลี่ยนโครงสร้างกลับมาเป็นทรานส์อีกครั้งเมื่อถูกกระตุ้นด้วยอุณหภูมิหรือแสง จากการศึกษาฤทธิ์ยับยั้งอนุมูลอิสระ โครงสร้างแบบทรานส์และซิสให้ผลที่ไม่แตกต่างกันอย่างมีนัยสำคัญ ทั้งออกซีเรสเวอราทรอลและเรสเวอราทรอล แต่ทรานส์ออกซีเรสเวอราทรอลแสดงฤทธิ์ยับยั้งเอนไซม์ไทโรซิเนสได้ดีกว่าโครงสร้าแบบซิส ส่วนเรสเวอราทรอลไม่แสดงฤทธิ์ยับยั้งเอนไซม์ไทโรซิเนส เมื่อทำการกักเก็บทรานส์ออกซีเรสเวอราทรอลลงในอนุภาคระดับนาโนเมตรโดยใช้เมทิลและเอทิลเซลลูโลสที่อัตราส่วนเซลลูโลสต่อทรานส์ออกซีเรสเวอราทรอล 2:1 พบว่าอนุภาคที่เตรียมได้มีขนาด 190 นาโนเมตร มีประสิทธิภาพการห่อหุ้ม 76% อนุภาคที่เตรียมได้นี้ สามารถควบคุมให้เกิดการปลดปล่อยทรานส์ออกซีเรสเวอราทรอลออกมาอย่างช้า ๆ ที่ pH 5.5 และจากการศึกษาด้วยกล้องจุลทรรศน์แบบคอนโฟคอลชนิดที่ใช้เลเซอร์ในการสแกน พบว่าอนุภาคที่กักเก็บทรานส์ออกซีเรสเวอราทรอลสามารถซึมผ่านผิวหนังบริเวณใบหูของหมูลงไปสะสมอยู่ที่บริเวณรอบรูขุมขน

ภาควิชา เคมี ลายมือชื่อนิสิต .....

สาขาวิชา เคมี ลายมือชื่อ อ.ที่ปรึกษาหลัก .....

ปีการศึกษา 2557

5572120323 : MAJOR CHEMISTRY
KEYWORDS: TRANS-OXYRESVERATROL / CIS-OXYRESVERATROL / ANTI-OXIDATION / ANTI-TYROSINASE / NANOENCAPSULATION

SARANYOO SORNKAMNIRD: STABILITY AND NANO-ENCAPSULATION OF OXYRESVERATROL. ADVISOR: ASST. PROF. PATTARA SAWASDEE, Ph.D., 87 pp.

The stilbene *trans*-oxyresveratrol is an active compound from the heartwoods of *Artocarpus Lakoocha*. Its stability towards light and temperature was studied compared to that of *trans*-resveratrol. The results revealed that *trans*-isomers of oxyresveratrol and resveratrol were stable towards the fluorescent light and temperature within 7 days. The UV-A radiation caused the isomerization from *trans*-isomer to be *cis*-isomer in oxyresveratrol faster than resveratrol. *Cis*-oxyresveratrol rapidly isomerized to be *trans*-oxyresveratrol *via* thermal process. In contrast to resveratrol, *cis*-resveratrol changed to be *trans*-resveratrol *via* both thermal and light pathways. Moreover, *trans*- and *cis*-isomers both of oxyresveratrol and resveratrol showed the same anti-oxidation activity. *Trans*-oxyresveratrol showed higher anti-tyrosinase activity than *cis*-oxyresveratrol while both isomers of resveratrol had low activity. *Trans*-oxyresveratrol-loaded nanospheres were prepared using ethyl- and methyl-cellulose blend as the polymeric shell material. The 2:1 ratio of cellulose blend and *trans*-oxyresveratrol gave nanospheres with the average size of 190 nm and the highest encapsulation efficiency percentage (76%). These preparing nanospheres showed a sustained release of *trans*-OXY at pH 5.5. In addition, *trans*-oxyresveratrol-loaded nanospheres can penetrated the skin barrier and accumulated at the hair folicles of the porcine ear detected by confocal laser scanning fluorescence microscopy.

Department: Chemistry Student's Signature .....
Field of Study: Chemistry Advisor's Signature .....
Academic Year: 2014

ACKNOWLEDGEMENTS

First of all, I would like to convey my sincere gratitude to Assistant Professor Pattara Sawasdee, Ph.D., my advisor, for her advice, assistance, and encouragement as well as any supports provided during the course of this research and my master degree student life.

My grateful thank also extends to the members of thesis committee consisting of Associate Professor Vudhichai Parasuk,Ph.D., Associate Professor Supason Wanichwecharungruang, Ph.D., and Assistant Professor Panya Sunintaboon, Ph.D., the external examiner from Department of Chemistry, Faculty of Science, Mahidol University for their valuable comments arising from the discussion.

My appreciation is also extended to Natural Products Research Unit, Department of Chemistry, Faculty of Science, Chulalongkorn University for the support of chemical and laboratory facilities and all members in the research unit for their friendship and help during the graduate study.

Finally, I would like to express my thankfulness to my parents and family members for their inspiration, understanding, great support and encouragement throughout the entire education.

CONTENTS

Page

Page

Page

LIST OF TABLES

LIST OF FIGURES

LIST OF ABBREVIATIONS

OXY	Oxyresveratrol
RES	Resveratrol
%	Percent
^{o}C	Degree Celsius
mW	Milliwatt
ml	Milliliter
µg	Microgram
µl	Microliter
nm	Nanometer
ppm	Parts per million
rpm	Revolution per minute
min	Minute
v/v	Volume by volume
w/w	Weight by weight
cP	Centipoise
Da	Dalton
MWCO	Molecular weight cut-off
DMSO	Dimethyl sulfoxide
DLS	Dynamic light scattering
SEM	Scanning electron microscope
TEM	Transmission electron microscope
EC	Ethyl cellulose
MC	Methyl cellulose
U	Unit
UV/Vis	Ultraviolet/Visible
NMR	Nuclear magnetic resonance
HPLC	High performance liquid chromatography
%EE	Percent of encapsulation efficiency
%loading	Percent of loading capacity

CHAPTER 1

INTRODUCTION

1.1 Introduction

Trans-oxyresveratrol (*Trans*-OXY, Figure 1.1) or *trans*-2,4,3',5'-tetrahydroxystilbene is a stilbenoid compound which consists of two aromatic rings joined by an ethylene bridge. *Trans*-oxyresveratrol was firstly discovered by Mongkolsuk *et al.* in 1957 from the heartwoods of *Artocarpus Lakoocha* Roxburge (Moraceae) [1]. The previous reports demonstrated that *trans*-OXY exhibited a variety of biological activities, including anti-tyrosinase [2], anti-oxidation [3], anti- herpes simplex virus [4] and anti-helmintic activities [1].

The ethylenic bridge of the core structure led to the *cis-trans* isomerization in stilbene. In the past, natural stilbenes which exhibited various pharmacological activities were mostly found in the *trans*-isomers. However, in recently, several *cis*-stilbenes obtained from synthesis or plant isolation and their bioactivities were found to be significantly different from those of *trans*-isomers [5, 6]. Moreover, the *cis-trans* isomerization is known to occur under the influence of light and temperature [7]. As we mentioned above, *trans*-OXY exhibited the high anti-tyrosinase and anti-oxidation properties which could be used as the active compounds for cosmetic products. But no studies have been examined the light and temperature stabilities of *trans*-OXY and also the bioactivities of *cis*-OXY. In additionally, *trans*-OXY is less solubility in water, thus utilization in cosmetic products is limited. To overcome this problem, nano-encapsulation technology is alternative way to solve this.

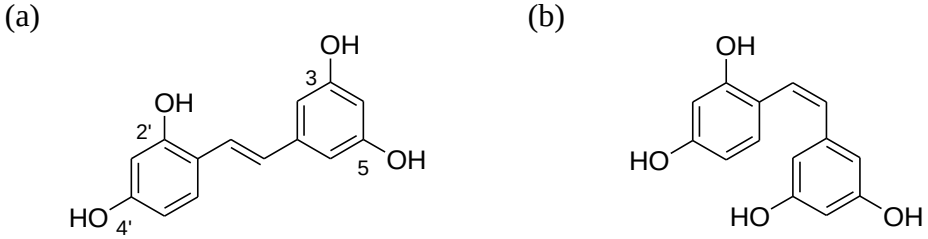

Figure 1-1 Chemical structures of (a) *trans*- and (b) *cis*-oxyresveratrol

Nano-encapsulation is a technology of packaging solids, liquids, or gaseous materials in particles with diameters of 1-1,000 nanometers. These particles could release their contents at controlled rates over prolonged periods. The materials that are entrapped may be called the active agent, internal phase or encapsulated

compound. Whereas those are used for encapsulated may be called shell, carrier material or wall material [8].

Nano-carriers aid for solubilizing hydrophobic drugs, decreasing drug clearance, controlling drug release and targeting drug delivery. Additionally, small particles can penetrate very effectively into the hair follicles. The particles can be used as an efficient carrier system for the transport of topically applied drugs into the reservoir of the hair follicles [9]. The drugs were released from the particles to penetrate independently through the targeting cell populations e.g. melanocytes. Melanocytes are melanin-producing cells located in the bottom layer of the skin's epidermis, and Melanin is the pigment primarily responsible for the skin color. In this study, *trans*-OXY was entrapped into nano-particles and tested for its penetration into the hair follicles. *Trans*-OXY released from particles and diffused to express the anti-tyrosinase activity at the melanocytes cells. Tyrosinase is a key enzyme in the biosynthetic pathway of melanin pigments in melanocytes cells [2].

There are many types of polymers for preparing the nano-particles e.g. cellulose, cellulose derivative, chitosan, and alginate. These polymers are biocompatible, safe and inexpensive. Cellulose derivatives, ethyl cellulose (EC) and methyl cellulose (MC), were chosen for encapsulating *trans*-OXY in this study. These polymers can fabricate through a self-assembling mechanism with an excellent loading capacity and high encapsulation efficiency [10]. Some of the hydroxyl groups on the repeating anhydroglucose units of EC and MC are modified into ethyl ether and methyl ether groups, respectively (Figure 1.2). Thus, EC is a hydrophobic cellulose, while MC is a hydrophilic cellulose.

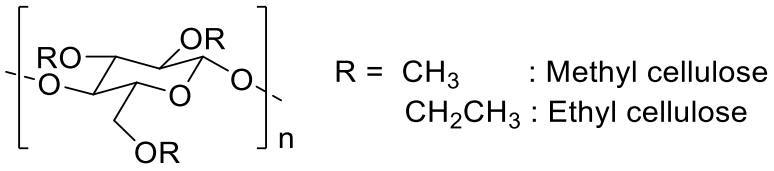

Figure 1-2 Chemical structures of methyl cellulose and ethyl cellulose.

1.2 The objectives of research

1. To study light and temperature stabilities of *trans*- and *cis*-OXY.

Trans-OXY was isolated from heartwoods of *Artocarpus Lakoocha* Roxburge (Moraceae) and characterized by ^{1}H and ^{13}C NMR spectroscopy. *Cis*-OXY was obtained by UV-A irradiation. The light stability in this study was investigated under UV-A and fluorescent lights whereas temperature stability was studied at room temperature, high

temperature (50 ºC) and low temperature (4 ºC). Moreover, resveratrol (RES), a known and popular stilbene, was also evaluated in the same experiments as OXY.

2. To study the anti-oxidation and anti-tyrosinase activities of OXY and RES.

Trans-OXY, *cis*-OXY, *trans*-RES and *cis*-RES were evaluated for their anti-tyrosinase and DPPH radical scavenging properties.

3. To prepare *trans*-OXY loaded cellulose derivatives nanoparticle.

Trans-OXY was encapsulated into nano-particle using ethyl cellulose (EC) and methyl cellulose (MC). The preparing nano-particles were characterized the morphology, size distribution, encapsulation efficiency, loading capacity, in *vitro* releasing and skin penetration.

CHAPTER 2
THEORY AND LITERATURE REVIEWS

Oxyresveratrol (OXY) possess several pharmacological and medicinal activities but it has low water solubility property. The water solubility property was a main problem for pharmaceutical uses. Therefore, water solubility improvement of OXY is important together with enhance its control release behaviors by encapsulation.

2.1 Oxyresveratrol

Oxyresveratrol is a major active compound of the heartwoods of Thai traditional plant, *Artocarpus lakoocha* Roxburgh (Moraceae) [11]. According to the folklore belief, boiling the heartwoods of *A. lakoocha* will obtained 'Puag-Haad' which used as an anthelmintic agent [2]. The principle compound in the Puag-Haad is *trans*-oxyresveratrol (*trans*-OXY). The previous studies reported that this compound possessed a wide spectrum of pharmacological properties; anti-herpes simplex virus (HSV)[4], anti-oxidation[12], and anti-tyrosinase[2] and neuroprotective[12] activities. Due to high inhibition towards tyrosinase and strong skin depigmenting effects in both animals and humans, *trans*-OXY is high potential to use as a skin-whitening agent in cosmetic products.

In 2007 Chuanasa *et al*. [4] reported that *trans*-OXY showed inhibitory effect on the growth of HSV-1 and HSV-2. *Trans*-OXY in vaseline was applied by topical treatment for five times daily provided better therapeutic efficacy than by oral treatment in cutaneous HSV-1 infection in mice. The combination of *trans*-OXY and acyclovir (a commercial drug for HSV infection treatment) produced synergistic anti-HSV-1 effect.

In 2003 Lorenz *et al.* [13] reported that *trans*-OXY is a more effective anti-oxidation than *trans*-RES or *trans*-4-hydroxystilbene in both DPPH reduction and nitric oxide scavenging capacity.

In 2012 Weber *et al.* [3] studied the potential neuroprotective effects of *trans*-OXY. They treated cell cultures (approximately 10% neurons and 90% glia as determined by immunohistochemistry experiments) with *trans*-OXY. The result showed that *trans*-OXY could prove to be a useful neuroprotective agent for traumatic brain injury.

In 2006 Likhitwitayawuid *et al.* [2] reported the tyrosinase inhibitory activity of *trans*-OXY and its derivatives. The result showed that *trans*-OXY and

2,4,3',5'-tetrahydroxybibenzyl showed significant strong tyrosinase inhibitory activity. Moreover, Shin *et al.* [14] indicated that *trans*-OXY inhibited the dopa oxidase activity of tyrosinase *via* a noncompetitive manner. *Trans*-OXY also showed higher inhibition on tyrosinase activities than kojic acid. The IC_{50} values of this activity of *trans*-OXY and kojic acid were 2.85 and 50.43 μg/ml, respectively.

In 2008 Chao *et al*. [12] showed that both pre-treatment and post-treatment SH-SY5Y neuroblastoma cells with *trans*-OXY significantly reduced the generation of intracellular reactive oxygen species triggered by 6-hydroxydopamine. This result suggested that *trans*-OXY may act as an intracellular antioxidant to reduce oxidative stress and was a potential nutritional candidate for protection against neurodegeneration in Parkinson disease.

2.2 Encapsulation

Encapsulation is a technology to entrap active agents within carrier materials. This technique is a useful tool to improve delivery of bioactive molecules such as foods or drugs [8]. Two main types of encapsulation particles were capsules and spheres (Figure 2.1). The capsules have a real shell surrounding the active agent. This type is also called reservoir, single-core, mono-core or core-shell types. Contrast to capsules, the spheres have no a real shell but the active agent disperses over the carrier material including at the surface of particles [15].

Encapsulation has many advantages including [16, 17]:

1. sustaining or prolonging drug release.
2. masking the unfavorable taste such as bitter or noxious drugs for their convenient handling.
3. converting volatile and oily substances or extracts into tabletted dosage forms to avoid tacky granulations and improve flow properties.
4. protecting drugs from environmental hazards such as humidity, light, oxygen or heat and gastrointestinal biodegradation.
5. enhancing compatibility between various drugs and excipients formulated together.
6. easy handling of hygroscopic and toxic substances such as fumigants, herbicides, insecticides and pesticides.

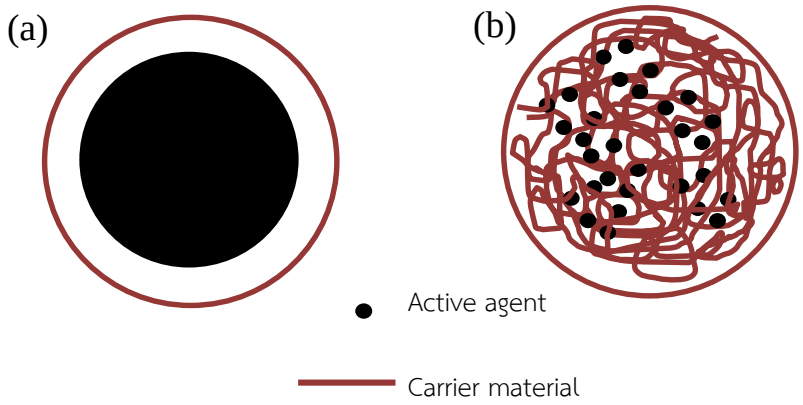

Figure 2-1 (a) Capsule and (b) sphere particles.

Nanoparticles were particles with have a size from 10 to 1000 nm. Over the past few decades, there has been considerable interest in developing biodegradable nanoparticles as effective drug delivery devices. Various polymers have been used in drug delivery research as they can effectively deliver the drug to a target site and thus increase the therapeutic benefit, while minimizing side effects. Liposomes have been used as potential drug carriers instead of conventional dosage forms because of their unique advantages which include ability to protect drugs from degradation, target the drug to the site of action and reduce the toxicity or side effects. However, developmental work on liposomes has been limited due to inherent problems such as low encapsulation efficiency, and poor storage stability. On the other hand, polymeric nanoparticles offer some advantages over liposomes [18]. Many polymers have been used to loaded drug or active molecule such as poly-lactide-co-glycolide [19-21], polylactic acid [22-25], poly-ε-caprolactone [26, 27],gelatin [28-30], chitosan [31-35], alginate [36-40] and cellulose derivative [41-45] etc.

Cellulose is the most common organic compound on the earth [46] and about 33% of all plant matter is cellulose. Cellulose consists of a linear chain of several hundred to over ten thousand glucose units by α-1,4 linkage. In contrast to that of starch, the glucose units of starch were linked by β-1,4 linkage. This bond makes cellulose linear, highly crystalline and indigestible for humans [47, 48]. Since cellulose is not absorbed systemically following oral administration, it has little toxic potential and is thus also a generally recognized as safe (GRAS) listed material. Cellulose is one of the most important pharmaceutical excipients and food it is a frequently used as tablet excipients [49]

Ethyl cellulose (EC) and methyl cellulose (MC)

Ethyl cellulose (EC, Figure 1.2) is derivative cellulose in which some of hydroxyl groups on the repeating glucose unit are converted to ethyl ether groups. EC has extremely been used for encapsulation due to its many versatile properties which are [16]

1. water insoluble but soluble in many organic solvents such as alcohol, ether, ketone and ester
2. biocompatible and compatible with many celluloses, resin and almost all plasticizers
3. stable against light, heat, oxygen and wetness and chemicals
4. non-toxic and non-irritant

EC particles have been prepared by single coating of EC around various chemical substances like drugs, pesticides, fragrances and food edibles. The interest of the scientific community in the EC has increased over the last years.

In 2011 Mirabedini *et al*. [50] prepared microcapsule containing plant oil by using EC as core polymer. It showed high yield and had a regular spherical shape with the diameter of 10–50 μm and the shell thickness of 0.65–1.55 μm.

In 2010 Zheng *et al.* [51] developed an oil dispersed phase method for preparing polyphenol containing microcapsules and using EC as wall material. The microcapsule had a smooth surface shape with a particle size distribution of 10–97 μm. Release rate of bayberry polyphenol from microcapsules was within the range of 2.56–15.14% under simulated gastric fluid.

In 2011 Feczk *et al.* [52] prepared ethyl cellulose nanocapsules containing a spirooxazine dye. The size of these nanocapsules is around 220 nm and the dye in the nanocapsules did not aggregate in a wide concentration range (0–30% w/w dye content).

In addition, drug release can be controlled and enhanced to some extent by addition of a water-soluble or water swellable polymer [53], e.g. hydroxypropyl methylcellulose and methyl cellulose.

Methyl cellulose (MC, Figure 1.2) is a natural carbohydrate polymer and freely soluble in water [54]. Blending different cellulose derivatives are often used for sustained release coatings. Moreover, enhancement of bioavailability of poorly water-soluble compounds is achieved by inclusion of the active principle in a faster dissolving hydrophilic excipient like ethyl/methyl cellulose blends. The changes in the porosity of the system allow a stable inclusion of poorly soluble molecules of an adapted size.

In 2006 Duarte *et al.* [55] prepared ethyl cellulose/methyl cellulose blends by the supercritical antisolvent (SAS) technique. SAS experiments were carried out at different pressure and temperature conditions. The preparing microspheres had the mean diameters ranging from 5 to 30 μm. The best process conditions for this mixture were at 40 °C and 80 bars.

In 2010 Suwannateep *et al.* [10] prepared nano-capsules encapsulated curcumin by dipolymeric EC and MC. It was easily fabricated through a self-assembling process and yielded the highest curcumin loading of 48.8%. It showed slowly release curcumin into the blood circulation for up to 3 h by orally administering in mice.

In 2010 Tunç and Duman [56] prepared MC and montmorillonite film for delivering and controlled releasing the carvacrol. The release rate of carvacrol from film was depended on the methyl cellulose to montmorillonite ratio and temperature.

2.3 Drug delivery and controlled release into the skin

Penetration of molecules and particles inside and through skin has long been well documented. There are a number of penetration routes through the stratum corneum barrier: the intercellular, intracellular and follicular pathways (Figure 2-2) [57]. The stratum corneum is hydrophobic layer has a 10–20 μm thick membrane consisting of dead cells (corneocytes) embedded in a lipid matrix.

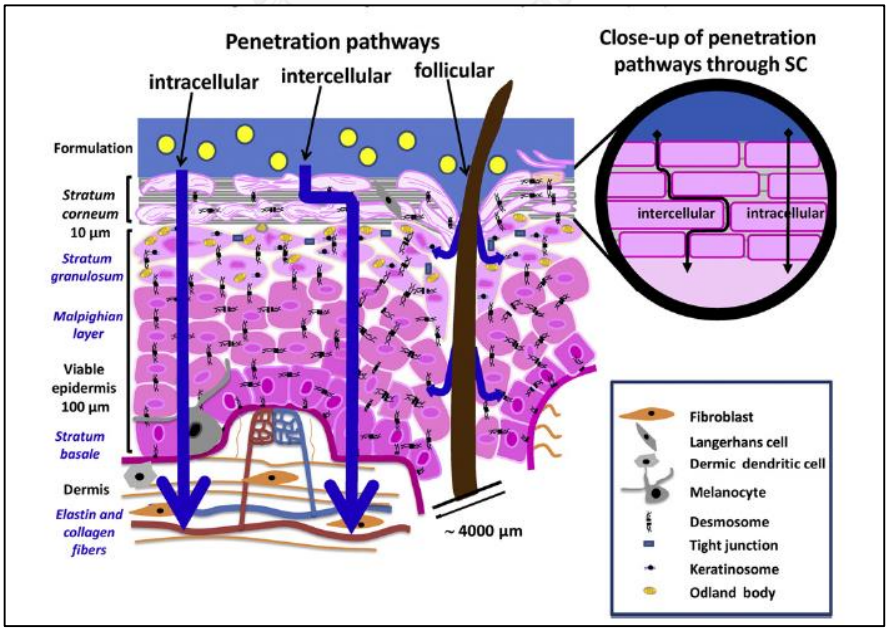

Figure 2-2 Possible transport pathways through the stratum corneum [57].

The intercellular pathway is appropriate for hydrophobic drugs, which was penetrate through the intercellular hydrophobic layer of stratum corneum. The intracellular pathway is suitable for hydrophilic molecules, which pass through the stratum corneum by the intracellular pathway through the corneocytes. The diffusion of drugs through skin may also occur through defects in the skin structure; for example, the hair shafts and sweat glands, which constitute break in the continuity of the stratum corneum, thus providing a follicular pathway [58].

Hair follicles represent an interesting target structure for drug delivery, since they are surrounded by a dense network of blood capillaries, which is important for uptake of topically applied drugs. Recently, it was demonstrated that particles in general and especially at a size between 300 and 643 nm penetrating very efficiently and deeper into the hair follicles than non-particulate substances [59, 60]. Likewise, the storage time was found to be increased by up to 10 days, in the case of the particulate substances, which is significantly longer than that of the non-particulate substances (4 days) [61].

Topically applied substances can follow different routes once they penetrate into hair follicles. Small drugs can penetrate through the follicular epithelium into the living tissue where they may be taken up by the blood circulation. Substances that were too large for penetration such as particles are entrapped within the hair follicles. They are depleted only by slow processes such as hair growth and sebum flow [62]. It is widely research in this subject e.g.:

In 2006 Vogt *et al*. [63] developed a vaccination strategy based on the ability of nanoparticles to penetrate hair follicles. A size-dependent internalization behavior of nanoparticles after topical application *in vitro* on human skin samples was revealed. Only 40 nm particles deeply penetrate into vellus hair openings and through the follicular epithelium.

In 2013 Subongkot *et al.* [64] elucidated the skin penetration pathway of the generated liposomes of limonene. They suggested that these liposomes might attach to any part of the skin before releasing the entrapped drug into the skin. Most liposomes and entrapped drug penetrated through hair follicles more than through the nonfollicular region. The follicular pathway was the major penetration pathway of liposomes with limonene for transdermal drug delivery, whereas the intercellular and intracellular pathways were the minor penetration pathways.

In 2014 Rancan *et al.* [65] investigated the stability and release properties of biodegradable polylactic acid particles upon topical application on human skin explants. Polylactic acid particles loaded with the hydrophilic fluorochrome 4-Di-2-Asp.

The particle average size was 207 nm. They found that particles maintained the particulate morphology, accumulated in hair follicles, and allowed a constant release of the incorporated fluorochrome for up to 16 h.

CHAPTER 3
EXPERIMENTAL

3.1 Chemicals and Materials

All chemicals and reagents were analytical grade. Standard *trans*-resveratrol (standard *trans*-RES), standard *trans*-oxyresveratrol (standard *trans*-OXY), ethyl cellulose (EC) (viscosity 100 cP; ethoxy content 48%) and methyl cellulose (MC) (viscosity 400 cP; Mn 40,000) were purchased from Sigma-Aldrich, St. Louis, USA. *Trans*-oxyresveratrol (*trans*-OXY) was isolated from the heartwoods of *Artocarpus lakoocha* Roxb. (Moraceae) which were collected from Uttaradit Province, Thailand, in June 2012.

Filtering centrifugal tube MWCO 100,000 (Amicon Ultra-15) was purchased from Millipore (Billerica, USA). Dialysis tubing cellulose membranes (MWCO 3,500 Da) was purchased from Sigma-Aldrich, St. Louis, USA.

Butylated hydroxytoluene (BHT), kojic acid, L-3,4-dihydroxyphenylalanine (L-DOPA), 1,1-Diphenyl-2-picrylhydrazyl (DPPH) and mushroom tyrosinase were purchased from Sigma-Aldrich, St. Louis, USA.

Acetone-d_6, ethanol, methanol, acetone and dichloromethane were purchased from Merck, Darmstadt, Germany.

3.2 Method

3.2.1 Extraction of *trans*-oxyresveratrol from the heartwood of *A. lakoocha.*

Trans-oxyresveratrol (*trans*-OXY) was purified from the dried heartwoods of *A. Lakoocha* that were collected in June 2012 from Uttaradit Province, Thailand. The fresh heartwoods were boiled with water for 3 h., and removed the heartwoods residue by filtration. The filtrate was continued boiling to remove water until a viscous extract was obtained. The extract was fractionated by vacuum liquid chromatography eluted with the gradient system of CH_2Cl_2 and acetone to afford 5 fractions (fr.1 to 5). Then fraction 3 was crystallized from a mixture of acetone and water to obtain *trans*-OXY. Isolated *trans*-OXY was confirmed its structure by UV-VIS spectroscopy (Agilent 8453, C-1103A), high performance liquid chromatography (HPLC:Waters Alliance 600), ^{1}H and ^{13}C NMR spectroscopic data comparing with those of standard *trans*-oxyresveratrol. ^{1}H NMR spectra of oxyresveratrol in acetone-d_6 was

recorded on a Varian NMR spectrometer operated at 400 MHz using pulse accumulating of 32 scans.

3.2.2 Stabilities study

3.2.2.1 Stability study of *trans*-oxyresveratrol and *trans*-resveratrol

3.2.2.1.1 Stability toward fluorescent light

The solution of *trans*-oxyresveratrol (2.0 mg of *trans*-resveratrol in 2.0 ml of acetone-d_6), was transferred into three NMR tubes. Tube A was determined the ^{1}H NMR spectra as fresh *trans*-OXY. Tubes B and C were protected from fluorescent light and exposed to fluorescent light respectively and all kept at room temperature (30 ^{o}C) for 7 days. The ^{1}H NMR spectra of B and C were compared with fresh *trans*-OXY solution (A). In case of *trans*-resveratrol, the experiment was done similarly.

3.2.2.1.2 Stability toward temperature

The solution of *trans*-oxyresveratrol (4.0 mg of *trans*-oxyresveratrol in 4.0 ml of acetone-d_6) was transferred into four NMR tubes. Tube A was determined the ^{1}H NMR spectra as fresh *trans*-OXY. Tubes B and C were incubated at 4 ºC and room temperature respectively which were all protected from fluorescent light for 7 days. Tube D was incubated at 50 ºC which was protected from fluorescent light for 24 h. The ^{1}H NMR spectra of B, C and D were compared with fresh *trans*-OXY solution (A). In case of *trans*-resveratrol, the experiment was done similarly.

3.2.2.1.3 Stability toward UV-A radiation

UV-A photo-isomerization experiment was performed with 1 mg/ml of *trans*-oxyresveratrol prepared in 5.0 ml acetone-d_6. Before irradiation, 0.5 ml of this solution was first taken for the measurement of ^{1}H NMR spectroscopic data. The remaining solution was transferred into a quart cuvette and exposed to a broadband UVA radiation (320–400 nm, generated by an F24T12/BL/HO (PUVA) lamp, irradiances measured using UVA-400 C power meter, National Biological Corporation, Twinsburg, OH, USA) operating with an intensity of 4.2 mW/cm^2. At appropriate times, a 0.5 ml aliquot was withdrawn to determine the ^{1}H NMR spectroscopic data. The %mole fraction of *trans*-isomer to *cis*-isomer was calculated based on the integrated peak area

(PA) of the ethylene proton signals of both isomers. The %mole fraction of *trans and cis* isomer (and resveratrol) was calculated using the following equation:

$$\%\text{mole fraction } of trans - \text{isomer} = \frac{\text{PA}_{trans}}{\text{PA}_{cis} + \text{PA}_{trans}} \times 100 \qquad \text{Eq. 3.1}$$

$$\%\text{mole fraction } of cis - \text{isomer} = \frac{\text{PA}_{cis}}{\text{PA}_{cis} + \text{PA}_{trans}} \times 100 \qquad \text{Eq. 3.2}$$

The signals of *cis*-OXY appeared at δ_H 6.55 (1H, *d*, *J*=8.3 Hz) and 7.02 (1H, *d*, *J*=8.3 Hz) ppm. However, the signal at δ_H 6.55 ppm was overlapped with other signals, the integrated peak area of signal at δ_H 7.02 ppm was only used for calculation. Meanwhile, that at δ_H 7.33 (1H, *d*, *J*=16.4 Hz) ppm of *trans*-isomer was used. In case of *trans*-RES, the same experiment as *trans*-OXY was done. And the integrated peak area of signals at δ_H 6.43 (1H, *d, J*=12.8 Hz) and 7.02 (1H, *d, J*=16.4 Hz) ppm of *cis*- and *trans*-isomers were used for calculation, respectively.

3.2.2.2 Stability study of *cis*-oxyresveratrol and *cis*-resveratrol

The solution of *cis* isomers were prepared by irradiating 1.0 mg/ml solution of *trans* isomers in acetone-d_6 with a broadband UVA radiation operating with an intensity of 4.2 mW/cm^2 for 1 h.

3.2.2.2.1 Stability toward fluorescent light

Cis-oxyresveratrol in acetone-d_6 was transferred into NMR tubes. Set A was exposed to fluorescent light and set B were protected from fluorescent light at room temperature. At appropriate times, a 0.5 ml aliquot was withdrawn to determine the ^{1}H NMR spectroscopic data. The %mole fraction of *trans and cis* isomer were calculated as mentioned in the effect of UV-A radiation evaluation (Eq. 3.1 and 3.2). *Cis*-RES was also studied accordingly.

3.2.2.2.2 Stability toward temperature

Cis-oxyresveratrol in acetone-d_6 was transferred into NMR tubes. Three sets of NMR tubes were incubated at 4 ºC, room temperature and 50 ºC separately. At appropriate times, a 0.5 ml aliquot was withdrawn to determine the ^{1}H NMR spectroscopic data. The %mole fraction of *trans and cis* isomer were calculated as

mentioned in the effect of UV-A radiation evaluation (Eq. 3.1 and 3.2). *Cis*-RES was also studied accordingly.

3.2.3 Bioactivities

3.2.3.1 Anti-oxidation activity

Radical scavenging activity of compound was measured by slightly modified method of E.W.C. Chan [66]. Assays were conducted in a 96-well microplate, a spectrophotometer reader (ELISA, Molecular Devices) being used to determine the absorbance at 517 nm. Samples were dissolved in methanol. Each well contained 50 μl of sample and 200 μl of 0.3 mM DPPH in methanol. The samples were kept in the dark for 30 min at room temperature and then the decrease in adsorption was measured. Results were compared with a control consisting of methanol in place of sample. Radical scavenging activity was determined at 517 nm by the follows:

$$\%\text{Inhibition} = \frac{A_{control} - A_{sample}}{A_{control}} \times 100 \qquad \text{Eq. 3.3}$$

Butylated hydroxytoluene (BHT) was used as positive control as it has very high radical scavenging activity. Values of the concentration of samples required to scavenge 50% of free-radicals or to prevent DPPH by 50% (IC_{50}) were calculated from the regression equations prepared from the concentration of samples and percentage inhibition of each system.

3.2.3.2 Anti- tyrosinase activity

Anti-tyrosinase activity of compound was measured by slightly modified method of E.W.C. Chan.[66] Assays were conducted in a 96-well microplate, a spectrophotometer reader being used to determine the absorbance at 490 nm. Samples were dissolved in methanol. Each well contained 40 μl of sample with 80 μl of phosphate buffer (0.1 M, pH 6.8), 40 μl of tyrosinase (200 units/ml) and 40 μl of L-DOPA (2.5 mM). The samples were incubated for 30 min at room temperature. Each sample was accompanied by a blank that had all the components except L-DOPA. Results were compared with a control consisting of methanol in place of sample. Tyrosinase inhibitory activity was determined at 490 nm by the Eq.3.3.

Kojic acid was used as positive control as it has very high Tyrosinase inhibitory activity. Values of the concentration of samples required to prevent tyrosinase by 50%

(IC_{50}) were calculated from the regression equations prepared from the concentration of samples and percentage inhibition of each system.

3.2.4 Encapsulation

3.2.4.1 Preparing *trans*-oxyresveratrol-loaded nanospheres

Trans-oxyresveratrol (*trans*-OXY) was loaded into nanoparticles by inducing the self-assembly of polymer, ethyl cellulose (EC) and ethyl cellulose (EC) methyl cellulose (MC) blending, in the presence of *trans*-OXY. Encapsulation of OXY was prepared by solvent displacement method through adding aqueous phase.[10]

For encapsulation of *trans*-OXY using ethyl cellulose (EC) polymer, encapsulation process was started by dissolving EC in ethanol at room temperature with continuous stirring until solution turned clear. The *trans*-OXY was dissolved in ethanol (0.5 ml) and then mixed with EC solution. After that DI water was dropped into the *trans*-OXY-EC solution with continuous stirring until the final volume reached 20 ml. The suspension was continuous stirred overnight to achieve equilibrium at room temperature before further investigation.

Encapsulation of *trans*-OXY into dipolymeric ECMC polymer blend (EC: MC of 1:1 by weight) encapsulation process was started by dissolving EC in ethanol at room temperature with continuous stirring until solution turned clear. At the same period of time, MC was dissolved in water. The *trans*-OXY dissolved in ethanol (0.5 ml) was mixed with EC solution and MC solution was successively added together. After that DI water was dropped into the *trans*-OXY-EC-MC solution with continuous stirring until the final volume reached 20 ml. The suspension was continuous stirred overnight to achieve equilibrium at room temperature before further investigation.

The resulting nanosphere suspension were subjected to determine its encapsulation efficiency, *trans*-OXY loading capacity, *in vitro* control release, *ex vivo* skin absorption of encapsulated *trans*-OXY and characterized by scanning electron microscopy (SEM), transmission electron microscopy (TEM) and dynamic light scattering (DLS).

3.2.4.2 Encapsulation efficiency (EE) and Loading capacity (LC)

To find the encapsulation efficiency, the suspension of *trans*-OXY-loading spheres (1 ml) was filtered through filtering centrifugal tube (MWCO 100,000 (Amicon Ultra-15)). Centrifugation was carried out on an Allegra 64R Avanti 30 (Beckman Coulter, Inc, Brea, USA). The obtained solid on the filter was soaked in 10 ml of ethanol for 2

h at room temperature to ensure that the entire *trans*-OXY was dissolved. Then, the ethanol solution was quantified for *trans*-OXY using UV-VIS spectrophotometer at 328 nm. The UV-VIS absorption spectra were acquired with a UV-VIS spectrophotometer (Agilent 8453, C-1103A) using a quartz cell with 1 cm path-length. The encapsulation efficiency (EE) and loading capacity (LC) were calculated using equation 3.4 and 3.5 respectively.

$$\%\mathrm{EE} = \frac{\text{Weight of encapsulated } trans\text{–OXY in the particles}}{\text{Weight of } trans\text{–OXY initially used}} \times 100 \qquad \text{Eq. 3.4}$$

$$\%\mathrm{LC} = \frac{\text{Weight of encapsulated } trans\text{–OXY in the particles}}{\text{Weight of the encapsulate } trans\text{–OXY+Weight of polymers}} \times 100 \qquad \text{Eq. 3.5}$$

3.2.4.3 Characterization of nanoparticles

3.2.4.3.1 Dynamic Light Scattering (DLS)

The mean hydrodynamic diameter, size distribution and zeta potential of *trans*-OXY-loading spheres were measured in distilled water at 25 ℃ on a Malvern 3000HSA Zetasizer (UK) based on the dynamic light scattering (DLS) techniques.

3.2.4.3.2 Scanning Electron Microscopy (SEM)

The morphology of the particles was examined by scanning electron micrograph (SEM). The suspension of nanospheres was diluted in distilled water and sonicated for 10 min. The sample was placed on a double-side sticking tape, air-dried and gold spray-coated before examined under scanning electron microscope (Phillips, XL30CP).

3.2.4.3.3 Transmission electron microscopy analysis (TEM)

The morphology of the particles was examined by transmission electron microscopy micrograph (TEM). TEM photographs were obtained using Tecnai 20 TWIN (FEI, USA) with an accelerating voltage of 200 kV. in conjunction with selected area electron diffraction (SAED). A glass slide was dipped into the obtained suspension to gain the dried smooth film of nanoparticles on surface of the glass slide.

3.2.4.4 *In vitro* release studies

The *in vitro* release of the *trans*-OXY from dipolymeric ECMC polymer blend nanoparticles (Batch 3) was carried out in 0.01M phosphate buffer solution pH 5.5 as release medium. Ten milliliters of the suspension of *trans*-OXY-loading spheres was put into the dialysis membrane bag (MWCO 3,500 Da) tied at both ends and placed into 500 ml of 0.01M phosphate buffer solution pH 5.5 and kept at 37 ± 0.1 °C with continuous stirring (at 100 rpm). Three milliliters of release medium were withdrawn at predetermined time intervals (0, 1, 2, 4, 6, 7, 8, and 24 h) and the same volume of phosphate buffer solution (37 °C) was replaced. The amount of released *trans*-OXY in withdrawn phosphate buffer solution was evaluated using UV-VIS Spectrophotometer at 37±0.1°C at 328 nm. A calibration curve of *trans*-OXY in phosphate buffer was used to quantify the amount of released *trans*-OXY. Three repetitions were performed for all samples. The percentage of released *trans*-OXY was calculated using the following equation:

$$\%Trans - \text{OXY released} = \frac{\text{Weight of encapsulated OXY in release medium}}{\text{Weight of encapsulated OXY}} \times 100 \qquad \text{Eq. 3.6}$$

The in vitro release of the unencapsulated trans-OXY was also studied. Ten milligrams of free *trans*-OXY dissolved in ethanol 500 μ l and mixed with 9.5 ml of DI water was put into the dialysis membrane bag and operated similarly as above.

3.2.4.5 *Ex vivo* skin absorption of encapsulated trans-OXY

The experiment was started by placing 10 μ l of the *trans*-OXY-loaded spheres (2,000 ppm of polymer and 1,000 ppm of *trans*-OXY) onto the stratum corneum surface of a porcine ear piece (1.00 cm^2 area). The porcine ear was obtained directly from the butcher from freshly slaughtered pigs. The final coverage of polymer and *trans*-OXY on the skin was 0.02 and 0.01 mg/cm−2, respectively. The sample was then kept at 25 °C for 2 h before analyzed by confocal laser scanning fluorescent microscopy (CLSFM, Nikon Digital Eclipse C1−Si equipped with Plan Apochromat VC 100x, Melles Griot Diode Laser and 85 YCA-series Laser at 405 nm, a Nikon TE2000-U microscope, a 32-channel-PMT-spectral-detector and Nikon-EZ-C1 Gold Version 3.80 software). Fluorescent spectral signals of *trans*-OXY that was activated by laser at 405

nm were collected from the skin tissue at various depths. Images are acquired point-by-point showing the three-dimensional of topologically complex objects. The obtained spectra of each pixel were then unmixed into *trans*-OXY and skin auto-fluorescent components based on the spectral database constructed from fluorescent spectra of *trans*-OXY and the skin tissue, through the Nikon-EZ-C1 software. Images indicating locations of *trans*-OXY in the skin tissue were then constructed using the obtained resolved signals.

3.3 Data analysis

All measurements were performed in triplicate in each experiment with the results presented as the mean ± 1 SD. Statistical analysis was performed by one-way ANOVA and a multiple comparison between sample pairs was determined by Duncan test. Statistical significance was accepted at probability value $P < 0.05$.

CHAPTER 4
RESULTS AND DISCUSSION

Trans-oxyresveratrol (OXY) used in this study was isolated from the heartwood of *Artocarpus lakoocha* Roxb. (Moraceae) and characterized by NMR spectroscopy. The study of light and temperature stabilities and bioactivities of *cis*- and *trans*-oxyresveratrol (OXY) was evaluated and compared with those of resveratrol (RES). Finally, *trans*-oxyresveratrol loaded cellulose nano-particles was prepared and characterized by spectroscopic methods.

4.1 Identification of *trans*-oxyresveratrol from the heartwood of *A. lakoocha.*

Trans-OXY was isolated from *A. lakoocha* as described in Section 3.2.1 of Chapter III**.** Its chemical structure was characterized by ^{1}H and ^{13}C NMR spectroscopy and compared these NMR data with those of a standard *trans*-OXY (Figures 4.1-4.2 and Table 4.1). Moreover, the UV-vis spectrum of the isolated *trans*-OXY showed the same pattern as that of the standard *trans*-OXY (Figure 4.3). The 97.3% purity of the isolated *trans*-OXY was evaluated by HPLC analysis (Figure 4.4).

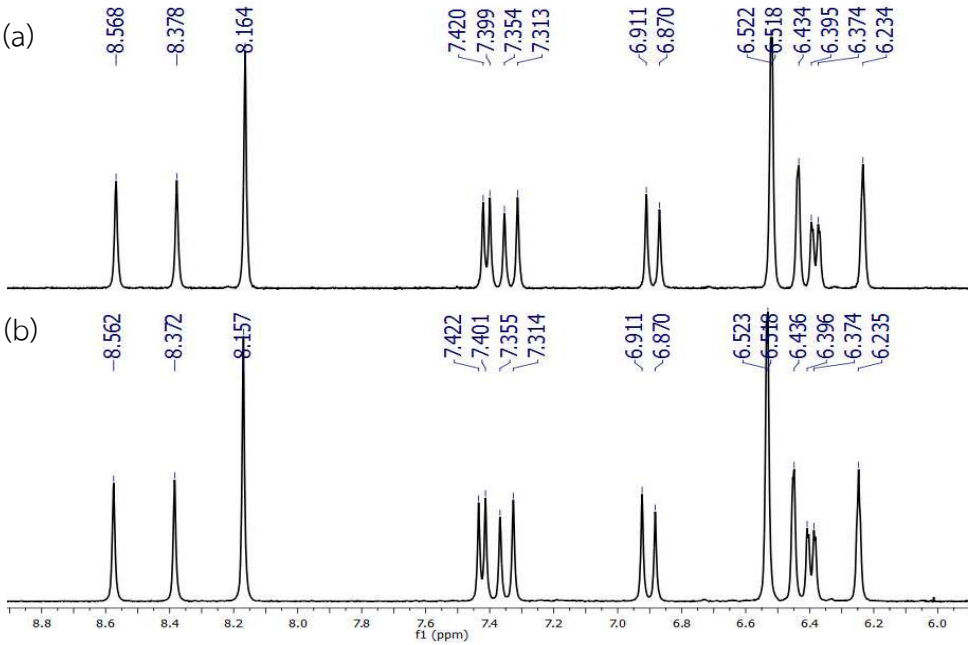

Figure 4-1 ^{1}H NMR spectra of (a) the isolated *trans*-OXY and (b) the standard *trans*-OXY.

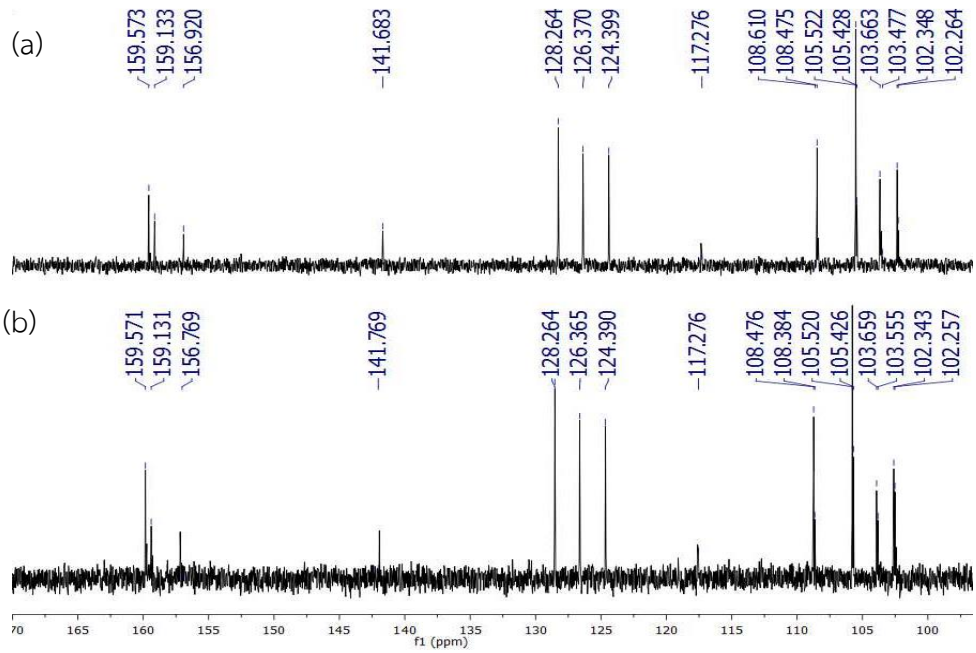

Figure 4-2 ^{13}C NMR spectra of (a) the isolated *trans*-OXY and (b) the standard *trans*-OXY.

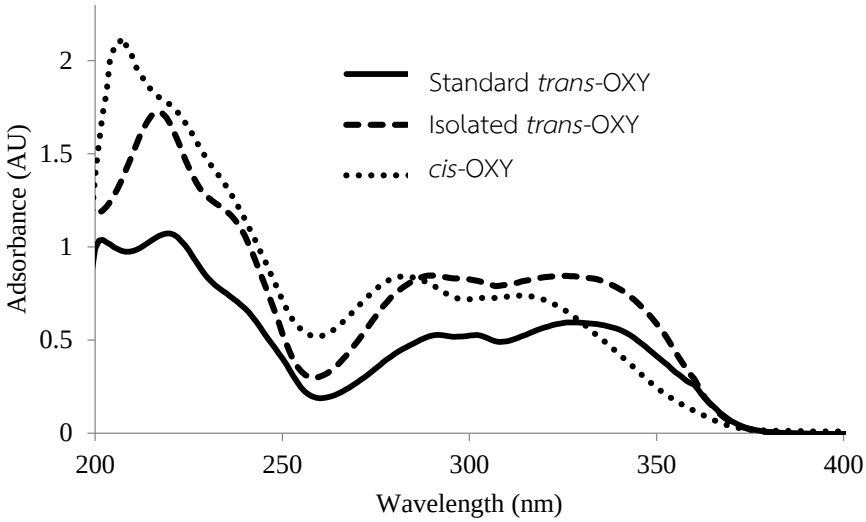

Figure 4-3 UV–vis absorption spectra of the standard *trans*-OXY, isolated *trans*-OXY and the *cis*-OXY in ethanol.

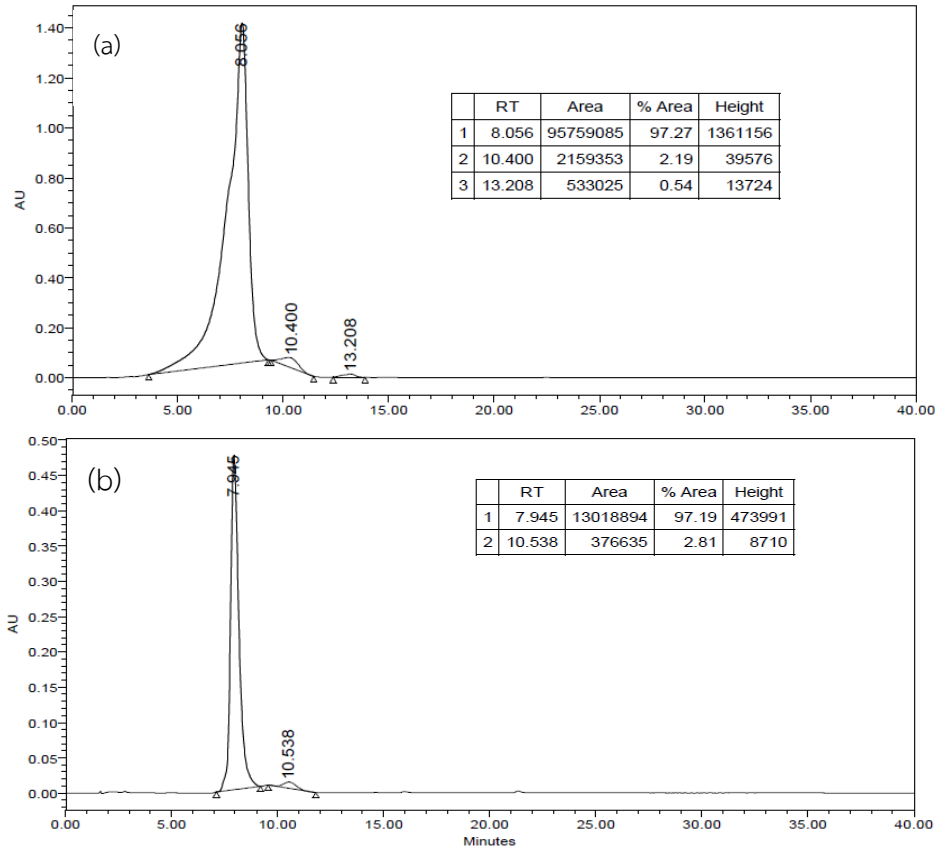

Figure 4-4 The HPLC chromatograms of (a) the isolated *trans*-OXY and (b) the standard *trans*-OXY.

Table 4-1 The ^{1}H and ^{13}C NMR chemical shift assignments of the isolated *trans*-oxyresveratrol (OXY) compared with those of the standard *trans*-oxyresveratrol.

Position	isolated *trans*-OXY		standard *trans*-OXY	
	δ_C	δ_H (int.,mult., *J* in Hz)	δ_C	δ_H (int.,mult., *J* in Hz)
1	141.7	-	141.7	-
2,6	105.5	6.52 (2H, *d*, 2.0)	105.5	6.52 (2H, *d*, 2.0)
3,5	159.6	-	159.6	-
4	102.3	6.24 (1H, *t*, 2.0)	102.3	6.24 (1H, *t*, 2.0)
a	128.7	6.89 (1H, *d*, 16.4)	128.3	6.89 (1H, *d*, 16.4)
b	126.4	7.33 (1H, *d*, 16.4)	126.4	7.33 (1H, *d*, 16.4)
1'	117.4	-	117.3	-
2'	156.9	-	156.9	-
3'	103.6	6.44 (1H, *d*, 1.6)	103.6	6.44 (1H, *d*, 1.6)
4'	159.1	-	159.1	-
5'	108.4	6.39 (1H, *dd*, 8.0, 1.8)	108.4	6.39 (1H, *dd*, 8.8, 2.6)
6'	124.4	7.41 (1H, *d*, 8.4)	124.4	7.41 (1H, *d*, 8.4)

4.2 Stability study of *trans*-oxyresveratrol and *trans*-resveratrol

4.2.1 Stability toward light

No signal change or shift in *trans*-OXY spectra was observed after exposing to the white fluorescent light at the room temperature for seven days (Fig. 4.5) while new signals were observed in *trans*-RES spectra. It was clearly that the new signals in Fig. 4.5b at δ_H 6.34 and 6.43 ppm were the signals of *cis*-ethylenic protons of *cis*-RES.

4.2.2 Stability toward temperature

Under darkness condition, *trans*-OXY and *trans*-RES were stable at 4 ^{o}C and room temperature for 7 days and at 50 ° C 1 days. No new or change signals appeared in those spectra of *trans*-OXY and *trans*-RES (Figs. 4.6)

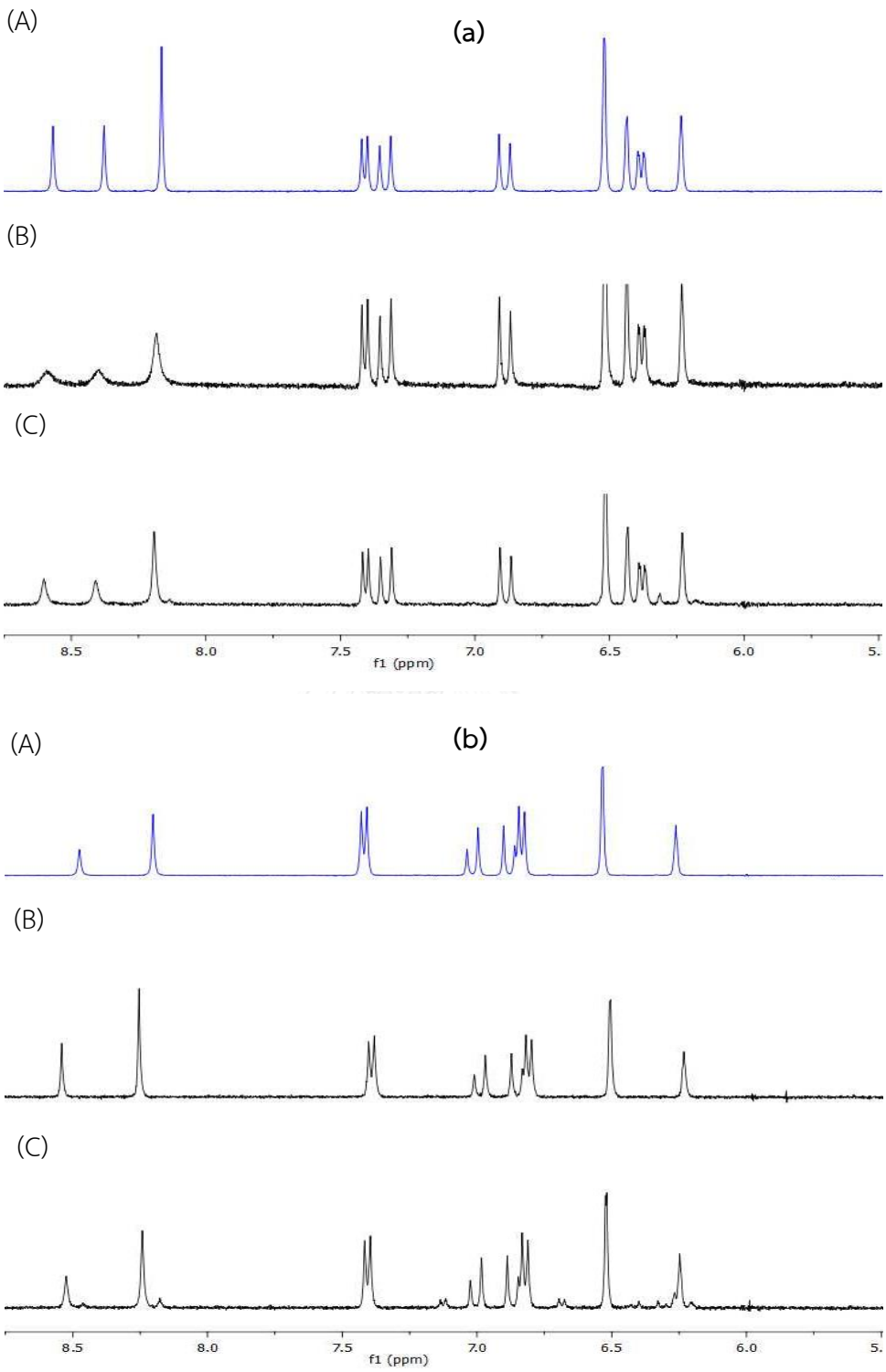

Figure 4-5 ^{1}H NMR spectra of the (a) *trans*-OXY and (b) *trans*-RES compared among (A) fresh *trans*-isomer, *trans*-isomer which were (B) fluorescent light protected and (C) fluorescent light exposed at room temperature for seven days.

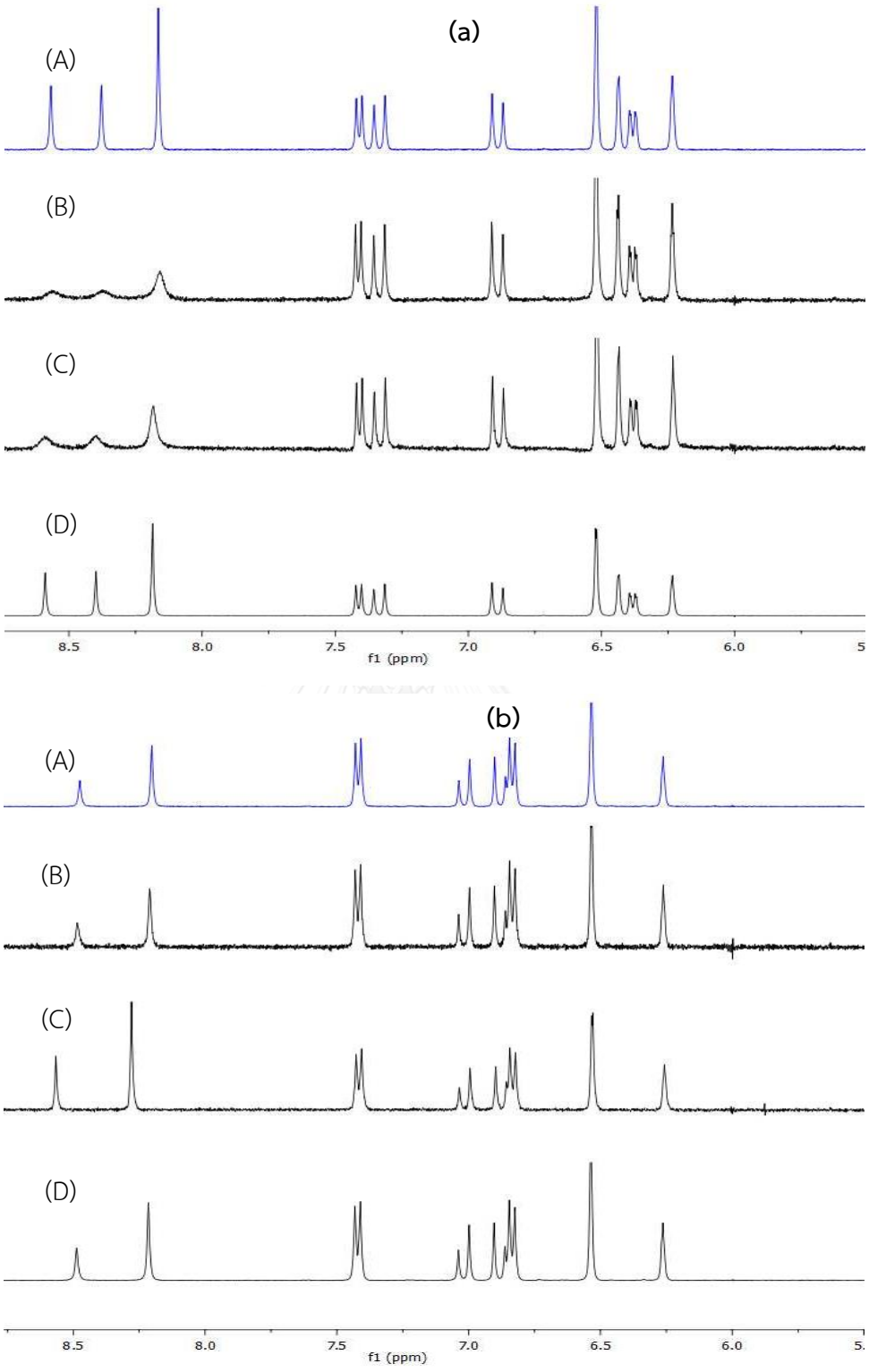

Figure 4-6 ^{1}H NMR spectra of the *trans*-OXY and *trans*-RES compared among (a) fresh *trans*-isomer, *trans*-isomer which were fluorescent light protected at (b) 4 °C, (c) the room temperature and (d) 50 °C.

4.2.3 Stability toward UV-A radiation

It has been known that *cis*-to-*trans* isomerization can occur when an isomer is exposed to UV radiation [67, 68]. In this study, the *trans*-isomers of both OXY and RES were exposed to the UV-A radiation (320–400 nm) and successive reduction in their ^{1}H NMR signals were observed when the exposure time increased. The new signal set of the *cis*-isomer appeared and increased as the function of radiation exposed time. The maximum conversion of *trans* to *cis* isomer of both OXY and RES was 80% (mole fraction) after exposing to the UV-A radiation for 30 and 50 min, respectively (Figs. 4.7).

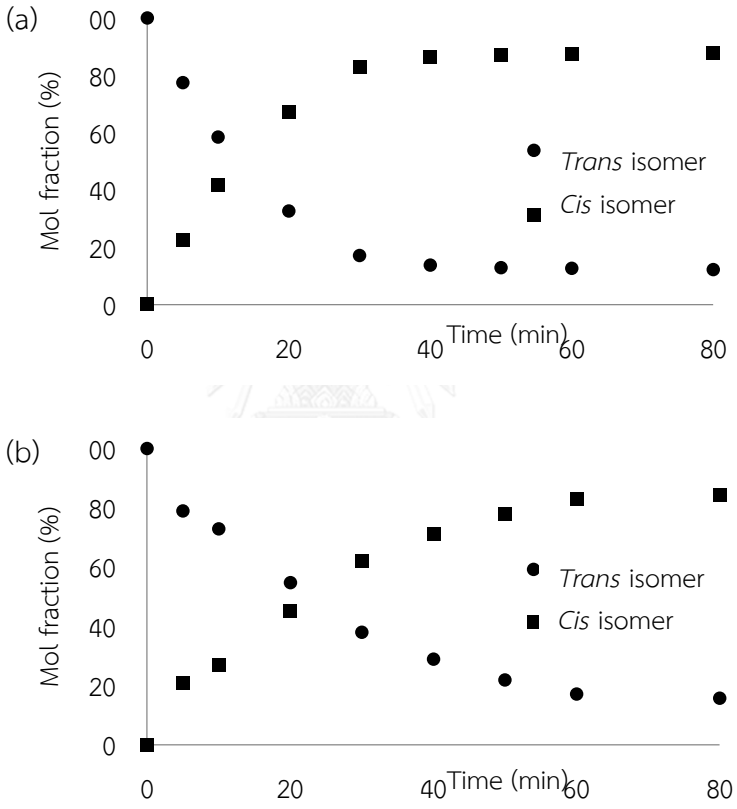

Figure 4-7 Mole fraction *trans* and *cis*-isomer at UVA irradiated various times of (a) OXY and (b) RES.

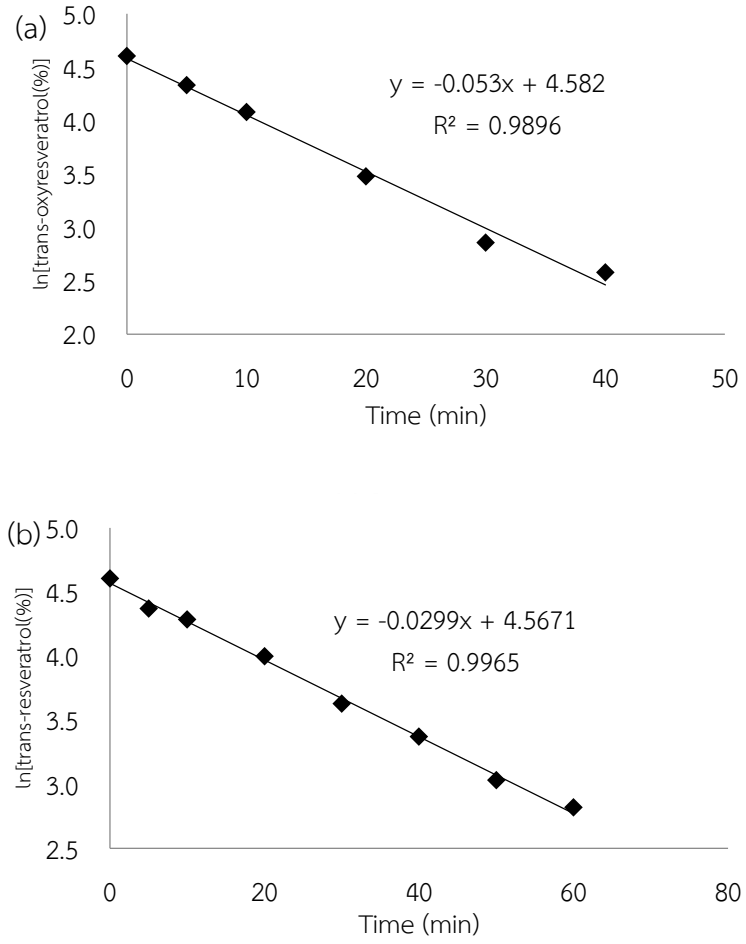

Figure 4-8 Determination of apparent rate constant (k) and half-life ($t_{\frac{1}{2}}$) of (a) *trans*-OXY and (b) *trans*-RES photo-isomerization based on first-order kinetics by ^{1}H NMR**.**

Trans-to-*cis* isomerization by UV-A irradiation or photo-isomerization is an intramolecular process and the rate of this reaction might be a first-order-reaction. Thus, the rate law of *cis-trans* isomerization could be presented as Eq. 4.1.

$$-\frac{d[A]}{dt} = k[A] \qquad \text{Eq. 4.1}$$

k is the rate constant and [A] is the concentration of reactant A.

The integrated rate law of Eq. 4.1 is showed in Eq. 4.2.

$$\ln [A]_t = -kt + \ln [A]_0 \qquad \text{Eq 4.2}$$

The plotting ln [*trans*-isomer (%)] versus irradiated time showed in Fig. 4.8. The slope of linear lines given the rate constant (k) were 0.053 and 0.030 min^{-1} for *trans*-OXY and *trans*-RES, respectively. These results could be indicated that *trans*-to-*cis* isomer of OXY was faster than that of RES.

The half-life ($t_{\frac{1}{2}}$) of a first-order reaction can be calculated by Eq. 4.3.

$$t_{\frac{1}{2}} = \frac{\ln 2}{k} \qquad \text{Eq 4.3}$$

The half-life of a reaction describes as the time needed for decreasing a half of the reactant. Calculation using Eq. 4.3, the half-life values of *trans*-OXY and *trans*-RES were 13 and 23 min, respectively (Fig. 4.8).

4.3 Stability study of *cis*-oxyresveratrol and *cis*-resveratrol.

Cis-OXY and *cis*-RES were obtained by irradiating *trans* isomer solution to a broadband UVA radiation (320–400 nm) operating with an intensity of 4.2 mW/cm^2 for 1 h.

4.3.1 Stability toward light

Effect of the fluorescent light on *cis*-structure of OXY and RES are shown in Figure 4.9. The decrease of *cis*-OXY seemed to be independent from the light while that of *cis*-RES was affected by the light. Moreover, *cis*-OXY isomerised to be *trans*-OXY faster than that observed in cis-RES. After 3 days, *cis*-RES remained 77% whereas *cis*-OXY had only 12% in the darkness condition.

The *cis*-isomer is less stable than *trans*-isomer because steric crowding of the *ortho* sites causes the phenyl groups to twist slightly out of coplanarity. *Cis*-OXY is less stable than *cis*-RES it might seem reasonable to suggest that there is a steric interaction from the *ortho* hydroxyl group of the *cis*-OXY.

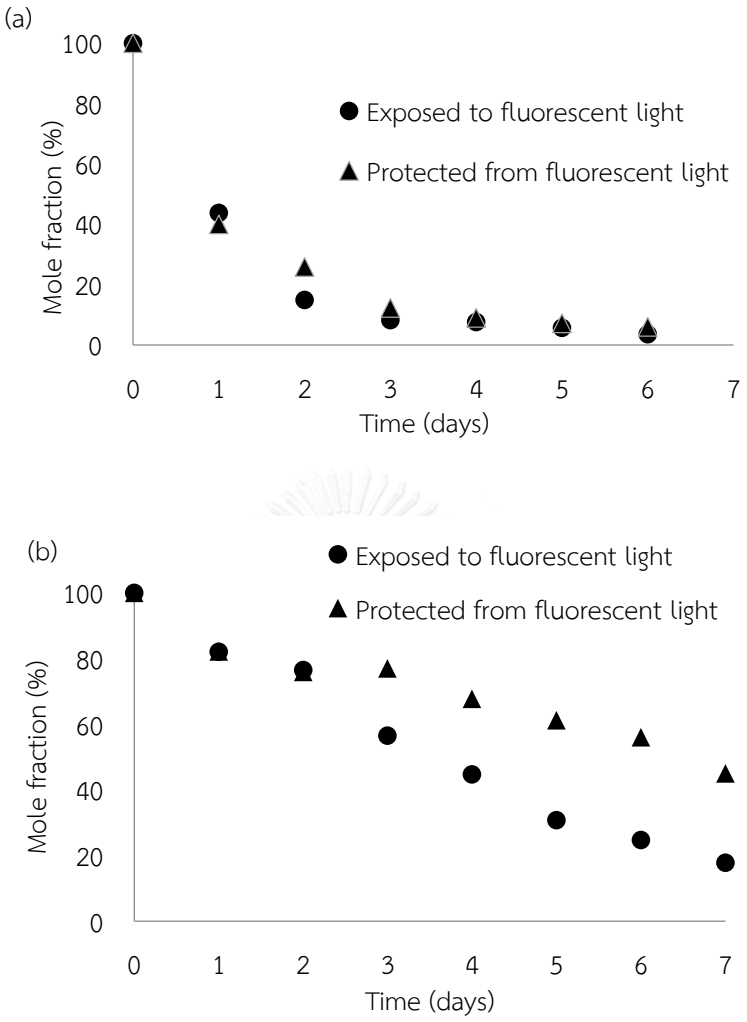

Figure 4-9 Mole fraction of *cis*-to-*trans* isomerization of (a) OXY and (b) RES as a function of time which exposed to fluorescent light and protected from fluorescent light at room temperature.

4.3.2 Stability toward temperature

The stability towards temperature of *cis*-OXY and *cis*-RES were investigated at 4 ℃, room temperature and 50℃. The relative percentage of *cis*-OXY over the time at various temperatures is shown in Figures 4.10 and 4.11. At 50℃, the rate of *cis*-to-*trans* isomerization of OXY was very fast. It remained only 5% after 24 h. In addition, the lower temperature significantly retarded this isomerization.

In contrast, *cis*-RES still remained up to 89% after 24 h at 50℃ and 54% after 6 days at the room temperature (Figures 4.12 and 4.13). The low temperature (4℃)

seemed to stop the isomerization of *cis*-RES in which 97% *cis*-RES were found after 20 days.

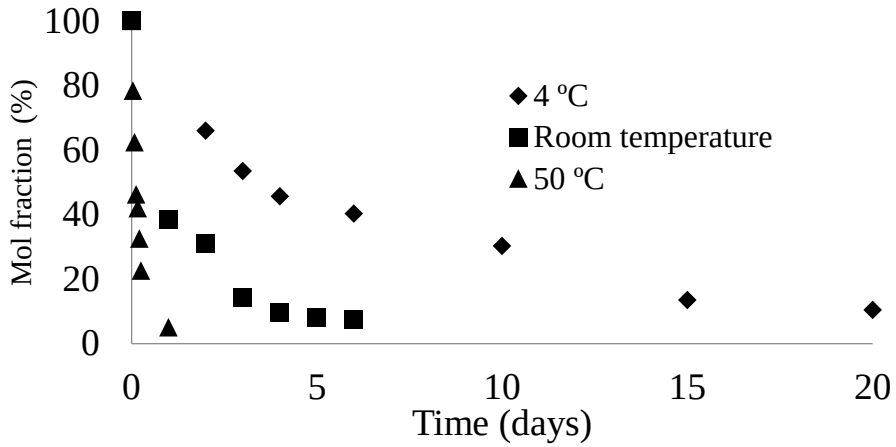

Figure 4-10 Mole fraction ratio of *cis*-to-*trans* OXY as a function of time at 4 °C, room temperature and 50 °C which were protected from fluorescent light.

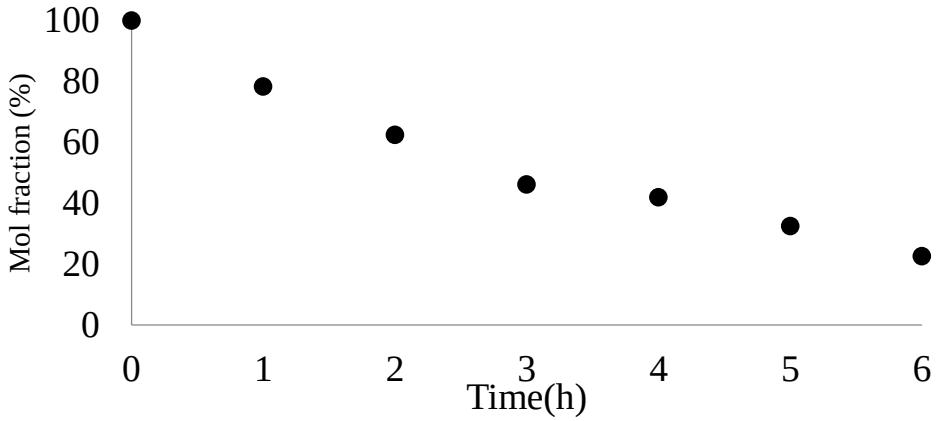

Figure 4-11 Mole fraction *cis*-to-*trans* OXY as a function of time at 50 °C under fluorescent light protection.

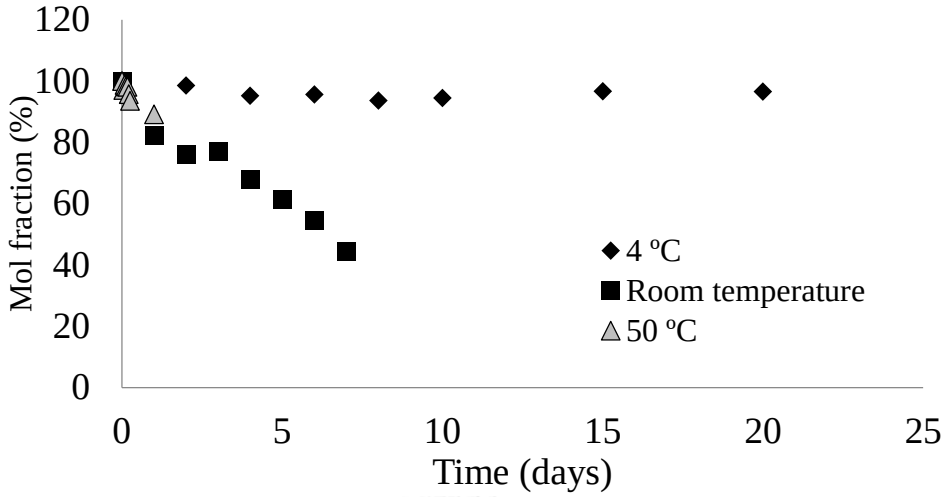

Figure 4-12 Mole fraction ratios of *cis*-to-*trans* RES as a function of time at 4 °C, room temperature and 50 °C under fluorescent light protection.

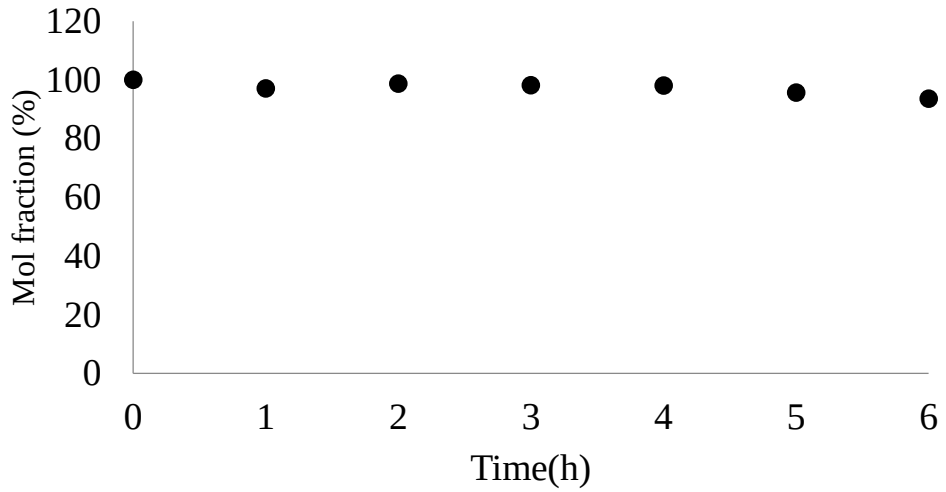

Figure 4-13 Mole fraction ratio of *cis*-to-*trans* RES as a function of time at 50ºC under fluorescent light protection.

4.4 Bioactivities

Trans-OXY was isolated from *A. lakoocha* and *trans*-RES was purchased from Sigma-Aldrich company. *Cis*-OXY and *cis*-RES were prepared by exposing *trans* isomer to UV-A radiation for 1 h. In this study, the average percentage of *cis*-OXY in the solution for bioactivity testing was 84% while that of *cis*-RES was 80%.

4.4.1 Anti-oxidation activity

The anti-oxidation potential was evaluated using the *in vitro* 1,1-diphenyl-2-picrylhydrazyl (DPPH) scavenging test. The free radical scavenging system is a proven assay in which anti-oxidants inhibit radical production. In the DPPH assay, the antioxidants were able to reduce the purple color of stable DPPH radical to the yellow color of 1,1-diphenyl-2-picrylhydrazine.

The IC_{50} values for *trans*-RES, *cis*-RES, *trans*-OXY, *cis*-OXY and a standard compound, butylated hydroxytoluene (BHT), were given in Table 4.2. These results revealed that all tested compounds showed higher scavenging DPPH radical than BHT, and OXY showed higher activity than RES. These results were in agreement with those previous reports in which the free radical-scavenging activity of polyphenols depends significantly on the number and position of hydroxyl groups, as well as conjugation and resonance effects [13]. OXY has four hydroxyl groups substituted on two aromatic rings whereas RES has only three hydroxyl groups. Moreover, hydroxyl group that substituted on *ortho*-position was extended delocalization and conjugation of the **π** electrons over aromatic rings, resulting in the high resonance stabilization of the hydroxyl radical formed in anti-oxidant reaction of the OXY (Figs. 4.14 and 4.15).

Table 4-2 Anti-oxidation and anti-tyrosinase activities of OXY and RES

Substance	IC_{50} ($\times 10^2$ μM)	
	Anti-oxidation	Anti-tyrosinase
BHT	5.75 ± 2.88^{a}	N/A
kojic acid	N/A	6.23 ± 1.16^{c}
trans-RES	4.50 ± 0.21^{a}	>40
cis-RES	3.37 ± 0.22^{a}	>40
trans-OXY	2.77 ± 0.26^{b}	0.32 ± 0.13^{d}
cis-OXY	2.74 ± 0.09^{b}	3.50 ± 0.90^{e}

N/A = not applicable

All values were based on three different samples. All assays were determined in triplicates and data presented as mean ± SD. For each column, values followed by the same letter (a–e) are not statistically different at P < 0.05 as measured by the Duncan test.

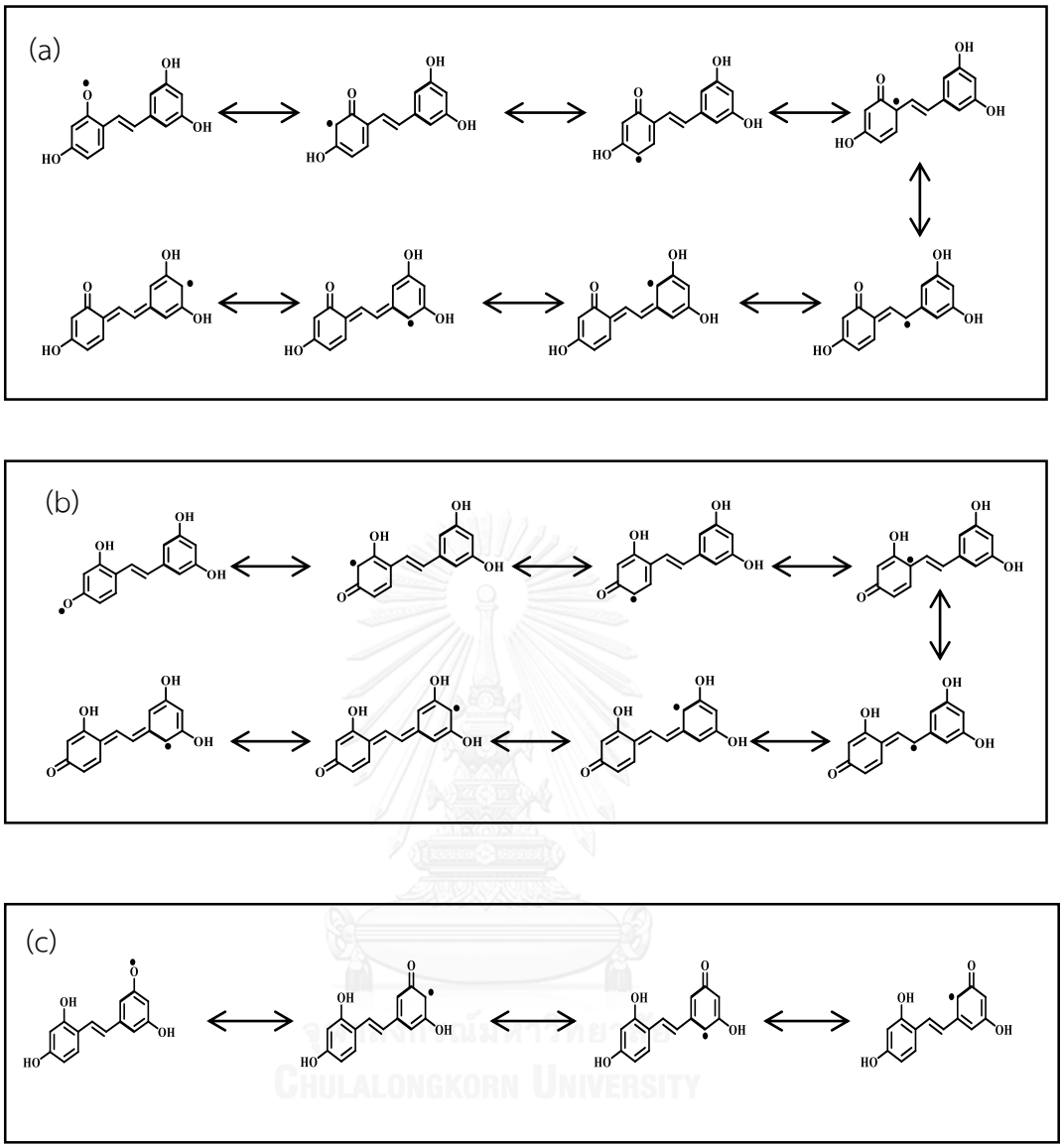

Figure 4-14 Resonance structures of hydroxyl radicals of *trans*-OXY at the (a) *ortho-*, (b) *para-* and (c) *meta*-position of *trans*-OXY.

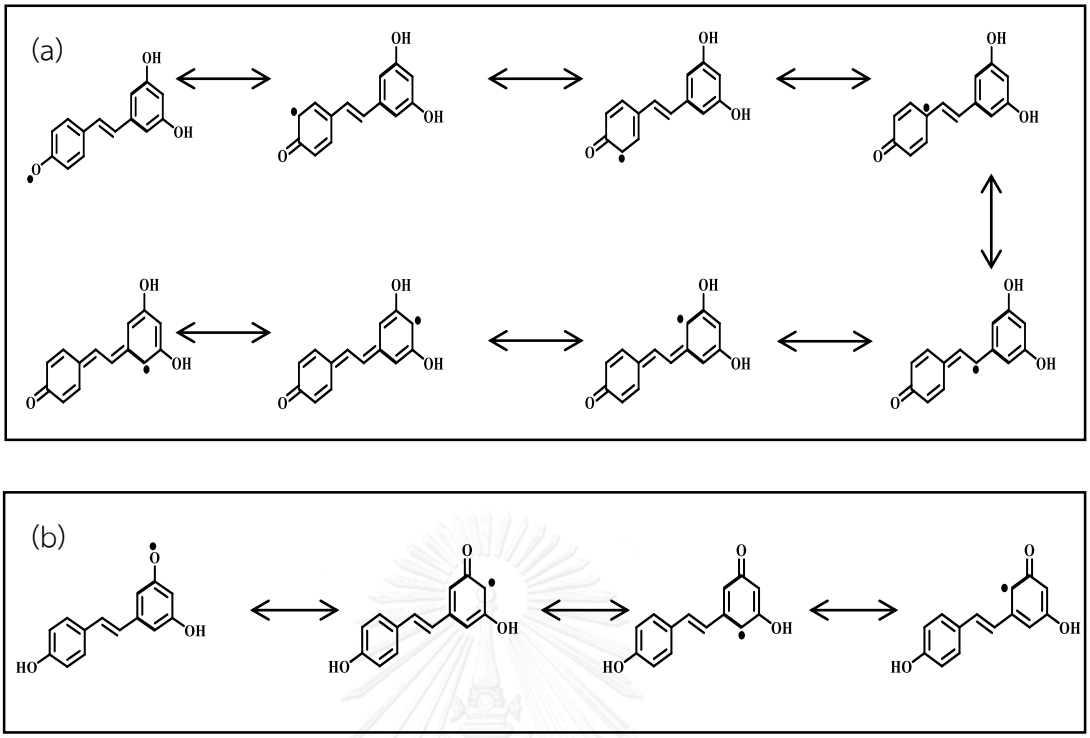

Figure 4-15 Resonance structures of phenoxyl radicals derived from *trans*-RES on (a) *para*- and (b) *meta*-position

4.4.2 Anti- tyrosinase activityin

Tyrosinase inhibitors are chemical agents which are capable of reducing some enzymatic reactions, such as food browning and melanisation of human skin. Tyrosinase inhibitors are not only used in medical treatment for hyper-pigmentation but also used in cosmetics products. The anti-tyrosinase effect was determined using the modified dopachrome method which L-DOPA was the substrate [66] and, in this study, kojic acid was used as a positive compound.

Among of tested samples, *trans*-OXY showed the highest tyrosinase inhibition with the IC_{50} value of 0.32×10^2 μM (Table 4.2). The *cis*-OXY had lower activity than *trans*-OXY but higher than kojic acid. On the other hands, RES isomers did not show mushroom tyrosinase inhibition even at the concentration of 1 mg/mL.

Trans- and *cis*-OXY showed the same activity on the anti-oxidation but significantly different on the tyrosinase inhibition. These might be that the radical scavenging potential is depending on the number of hydroxyl groups on the phenyl rings. In contrast, the tyrosinase inhibition is depend on the suitable conformation of inhibitors to bind at the active site of enzyme.

4.5 Encapsulation

4.5.1 Preparing *trans*-oxyresveratrol-loaded nanospheres

Trans-OXY-loaded cellulose nanospheres were prepared by the solvent displacement method. *Trans*-OXY was loaded into polymeric nanospheres *via* self-assembling process. Herein, ethyl cellulose (EC) and methyl cellulose (MC) were used as the carriers. During solvent displacement process in the distilled water, ethanol displaced by water. The hydrophobic *trans*-OXY was then interacted with the hydrophobic moiety of EC and MC. While hydrophilic moiety of EC and MC pointed toward the outer surface to interact with water molecules. This led to the self-assembly and obtain nanosphere suspension.

The physicochemical properties of *trans*-OXY-loaded only EC or EC and MC blend nanospheres were showed in Table 4.3. Batch 3 had the highest encapsulation efficiency (EE) and the smallest spheres. The SEM and TEM pictures showed that the particles of all batches were spherical in shape and nanoscale size (Figs. 4.16 and 4.17). Dynamic light scattering was used to analyze size and zeta potential of the particles, the results showed in Fig 4.18. These results are in good agreement with the particle size morphology given by SEM and TEM techniques.

Table 4-3 Physicochemical properties of *trans*-OXY-loaded nanospheres. Data were shown as the mean ± 1SD and are derived from 3 independent repeats.

Batch	Amount of EC (mg)	Amount of MC (mg)	Amount of *trans*-OXY (mg)	Weight ratio of EC:MC	Weight ratio of polymer: *trans*-OXY	%EE	%LC	Hydrodynamic diameter (nm)	Polydispersity index (PDI)	Zeta potential (mV)
1	40	-	20	1:0	2:1	59.7±2.2	23.0±0.7	241.8±4.6	0.094±0.061	-22.4±0.7
2	30	-	30	1:0	1:1	48.6±1.8	32.7±0.8	234.7±2.7	0.087±0.004	-25.3±0.3
3	20	20	20	1:1	2:1	76.0±2.8	27.5±0.7	190.1±1.9	0.083±0.002	-7.9±0.3
4	15	15	30	1:1	1:1	55.3±1.5	35.6±0.6	298.0±0.6	0.121±0.028	-10.7±0.3

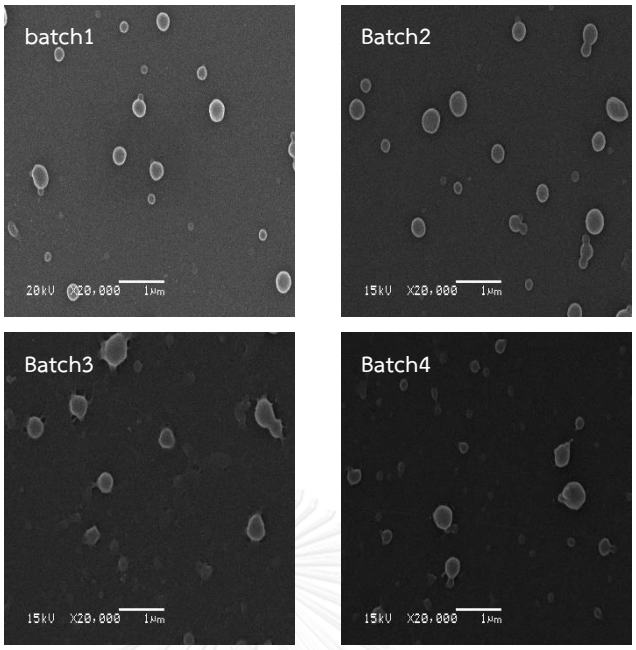

Figure 4-16 SEM photographs of *trans*-OXY-loaded nanospheres.

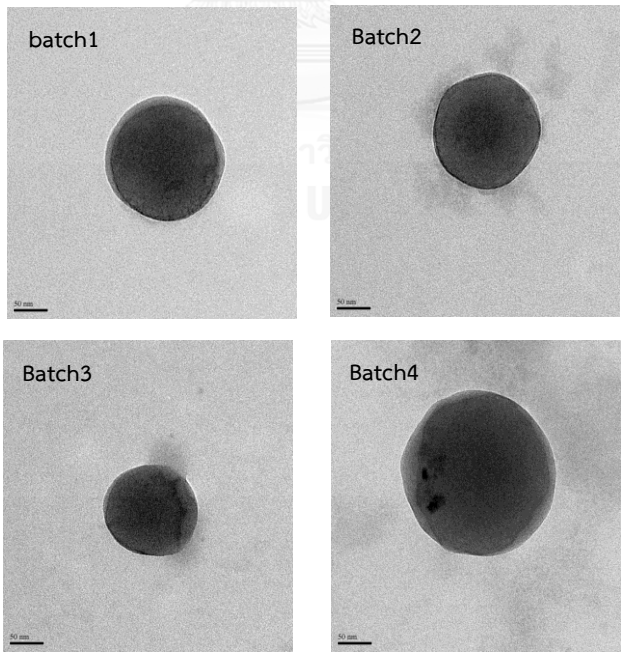

Figure 4-17 TEM photographs of *trans*-OXY-loaded nanospheres.

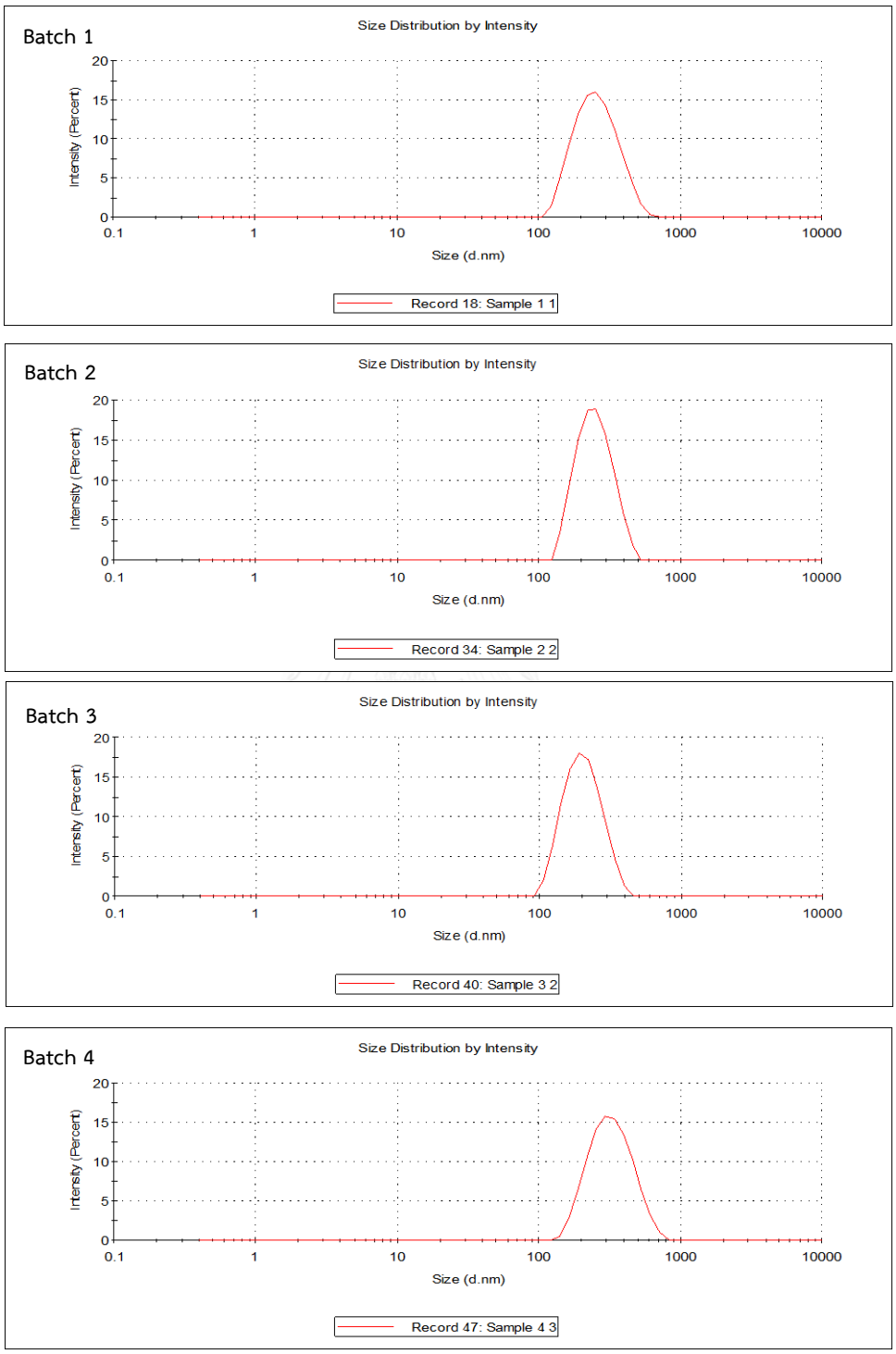

Figure 4-18 Size distributions of *trans*-OXY-loaded nanospheres.

4.5.2 *In vitro* release studies

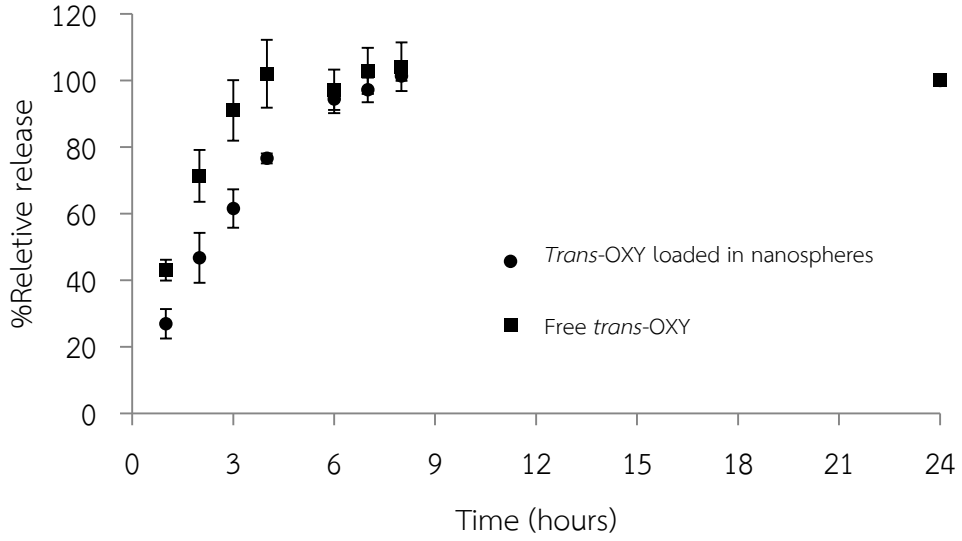

Figure 4-19 *In vitro* release of *trans*-OXY loaded in nanospheres and free *trans*-OXY in phosphate buffer solution (pH 5.5). Data were shown as the mean ±1SD and are derived from 3 independent repeats.

According to the highest EE, Batch 3 was chosen to further study the controlled release. The release of *trans*-OXY from nanospheres was evaluated in phosphate buffer solution pH 5.5 which mimic acidic environment of human skin, for 24 hours. In this condition, encapsulation obviously helped retarding the release of *trans*-OXY (Figure 4.19). The result also implied that nanoparticles fabricated from a blend of EC and MC was stable in acidic environment. In summary, nanospheres drug delivery system using a blend of EC and MC could sustain the release of *trans*-OXY, and this carrier was also stable in acidic environment. Thus, *trans*-OXY -loaded nanospheres might be a new therapeutic method for skin target. The carrier septum seems to be suitable for skin because the resident time of *trans*-OXY in hair follicles can be prolonged.

4.5.3 *Ex vivo* skin absorption of *trans*-OXY-loaded nanospheres

Confocal Laser Scanning Fluorescence Microscopy (CLSFM) is an alternative technique to study the skin penetration and distribution of model fluorescent compounds. CLSM using a co-localization technique can be applied to study the location of *trans*-OXY nanospheres on the skin in terms of attachment. During scanning, the confocal volume element is moved through a specimen by a succession of skin layers. By a defined focusing along the z-axis (axial direction), lateral movement is possible to image any object plane of interest within a specimen. The objective plane, as a whole, is recorded in a point-by point and line-by-line raster [69]. This technique employed the difference of fluorescence signals among *trans*-OXY and skin to indicate position of *trans*-OXY on the skin.

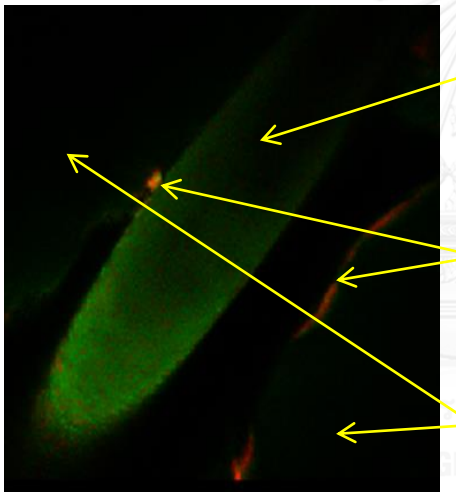

Figure 4-20 Confocal fluorescent microscopy images showed the optical image follicular region. The positions of red and green fluorescence represent *trans*-OXY and skin, respectively.

The obtained fluorescent signals from selected area were then deconvoluted for fluorescent spectra of *trans*-OXY and skin. The fluorescent signal of *trans*-OXY showed in red color and the fluorescent signal of hair showed in green color. Top view images in terms of depth of porcine ear treated with *trans*-OXY loaded nanospheres was presented in Figs 4.20 and 4.21. These figure shows that deposition was found surround at the hair follicle and presence of *trans*-OXY in the tissue. This investigation indicated that *trans*-OXY nanospheres can penetrate through skin and the hair follicles are a major pathway. Then *trans*-OXY diffuse through the skin tissue to prolong the absorption and sustained release of drugs through the skin, with prolonged therapeutic levels.

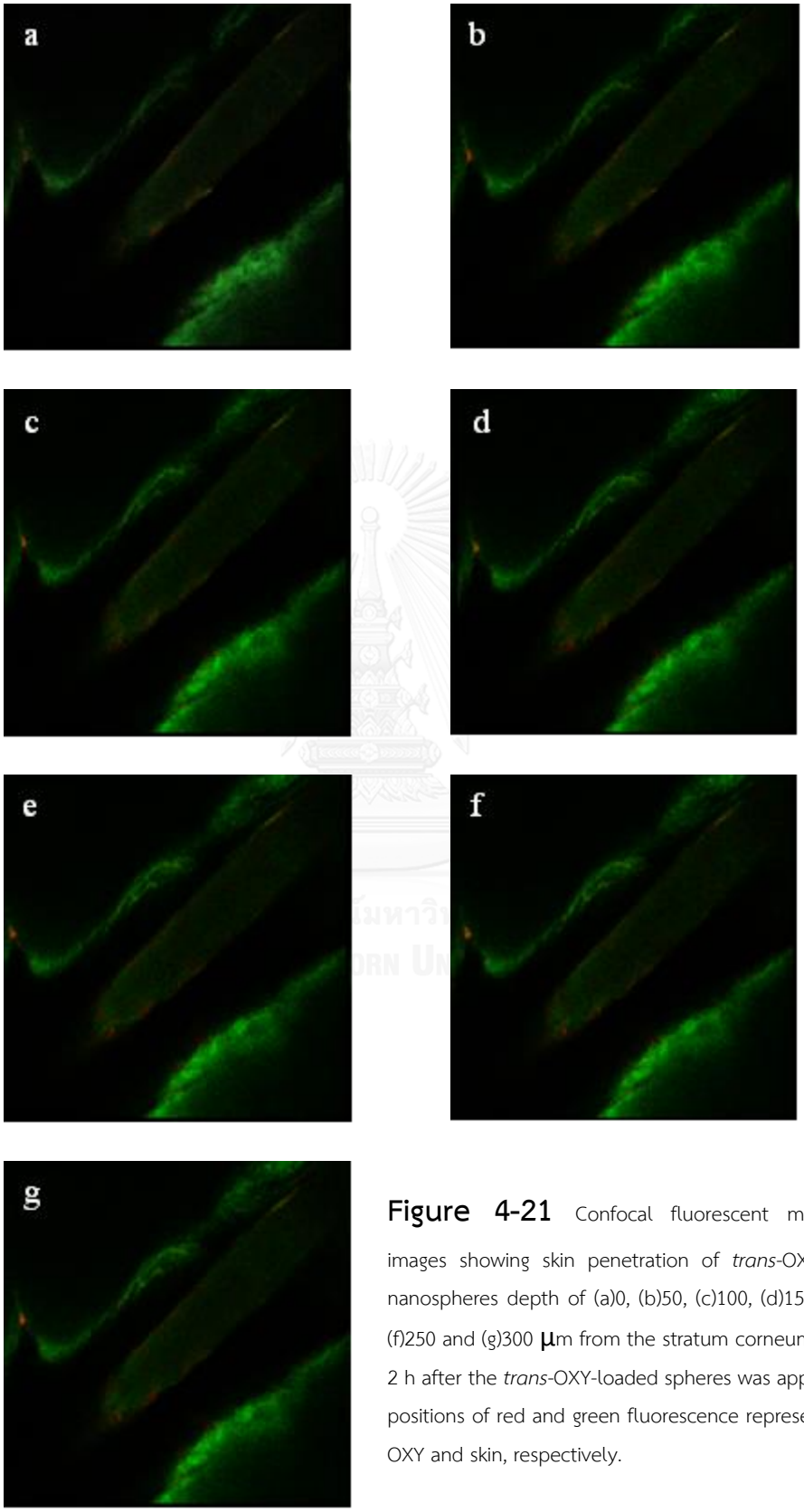

Figure 4-21 Confocal fluorescent microscopy images showing skin penetration of *trans*-OXY-loaded nanospheres depth of (a)0, (b)50, (c)100, (d)150, (e)200, (f)250 and (g)300 μm from the stratum corneum surface, 2 h after the *trans*-OXY-loaded spheres was applied. The positions of red and green fluorescence represent *trans*-OXY and skin, respectively.

CHAPTER 5

CONCLUSION

Trans-isomers of OXY and RES were stable towards the fluorescent light and temperature for at least 7 days. The UV-A irradiation caused the photo-isomerization of *trans*-OXY to be *cis*-OXY faster than that of trans-RES. *Cis*-OXY seemed to be unstable, it isomerized rapidly to be *trans*-OXY even in dark condition, it was changed approximately 90% to be *trans*-OXY within 3 days at room temperature. However, the low temperature can extend the *cis*-to-*trans* isomerization of OXY. *Cis*-RES isomerized slower than *cis*-OXY at room temperature and the conversion rate was influenced by the fluorescent light and temperature. The anti-oxidation activity of *trans*-isomer was closer to that of *cis*-isomer both OXY and RES. These results revealed that all tested compounds showed higher scavenging DPPH radical than BHT, and OXY showed higher activity than RES. The anti-tyrosinase activity of *trans*-OXY is the higher than *cis* form thay may be depend on the suitable conformation of inhibitors to bind at the active site of enzyme.

Trans-OXY was further encapsulated in ethyl- and methyl-cellulose blend. *Trans*-OXY-loaded nanospheres *trans*-OXY:EC:MC ratio is 1:1:1 is the best condition. The %EE, %LC and average size were 76, 28 and, 190 nm respectively. The *trans*-OXY-loaded EC/MC nanospheres show a sustained release of *trans*-OXY at pH 5.5. In addition, *trans*-OXY-loaded nanospheres can penetrate the skin barrier and accumulated at the hair folicle of the porcine ear detected by confocal laser scanning fluorescence microscopy.

APPENDIXES

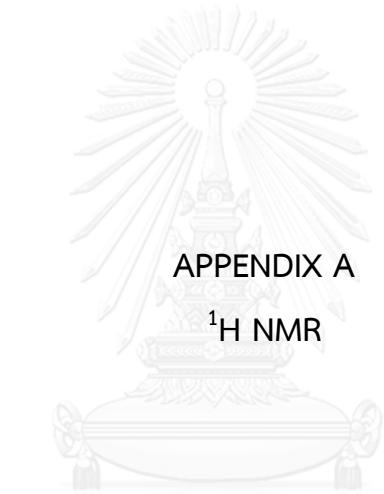

APPENDIX A

^{1}H NMR

^{1}H NMR

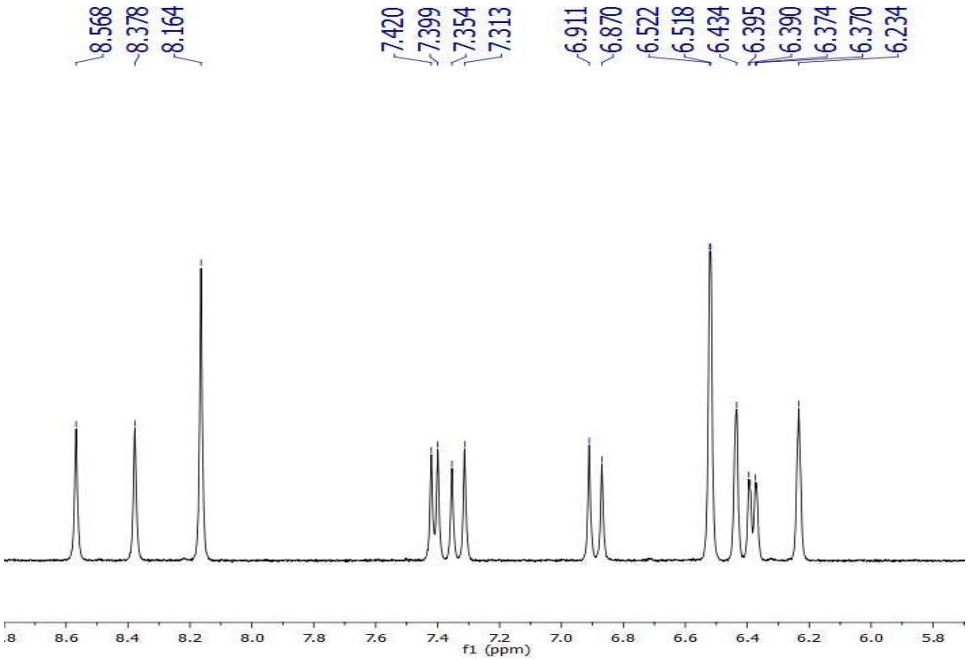

Figure A-1 ^{1}H NMR spectra of isolated *trans*-OXY.

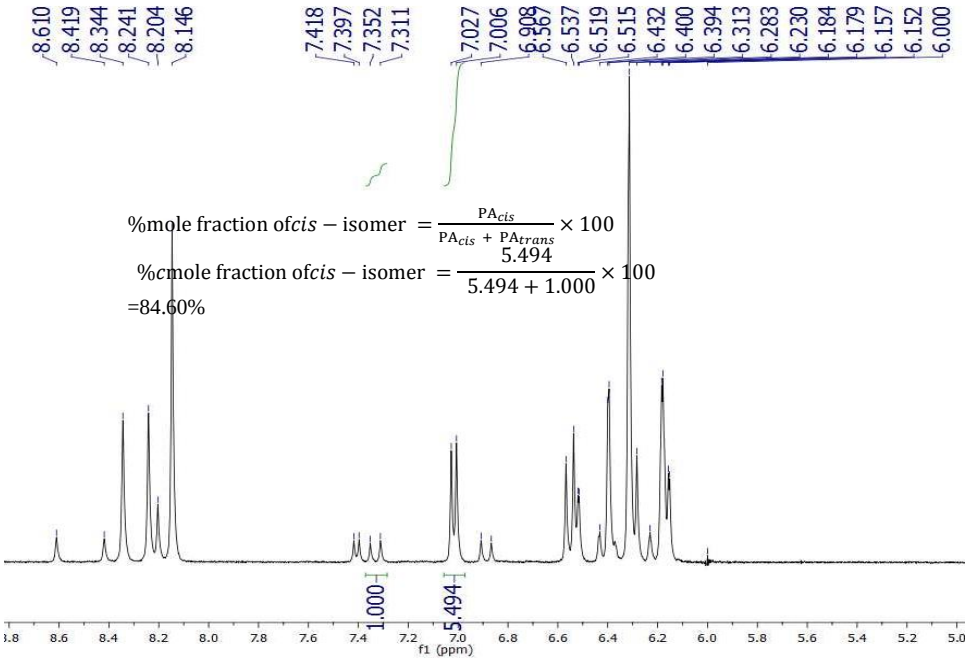

$$\%\text{mole fraction of} cis - \text{isomer} = \frac{\text{PA}_{cis}}{\text{PA}_{cis} + \text{PA}_{trans}} \times 100$$

$$\%c\text{mole fraction of} cis - \text{isomer} = \frac{5.494}{5.494 + 1.000} \times 100$$

=84.60%

Figure A-2 ^{1}H NMR spectra of the mixture of *trans*- and *cis*-OXY.

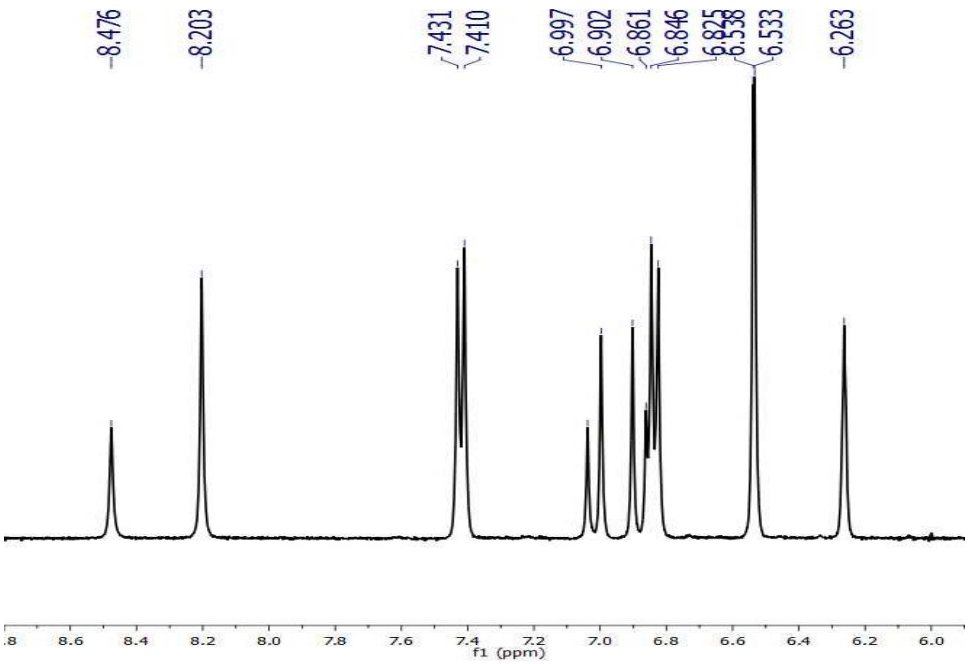

Figure A-3 ^{1}H NMR spectra of *trans*-RES.

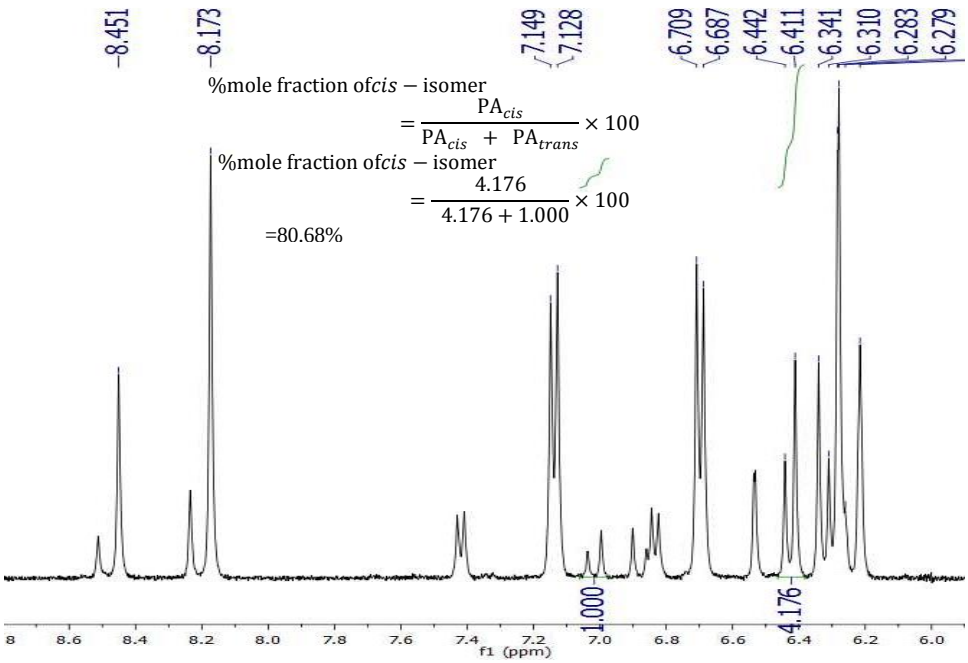

Figure A-4 ^{1}H NMR spectra of the mixture of *trans*- and *cis*-RES.

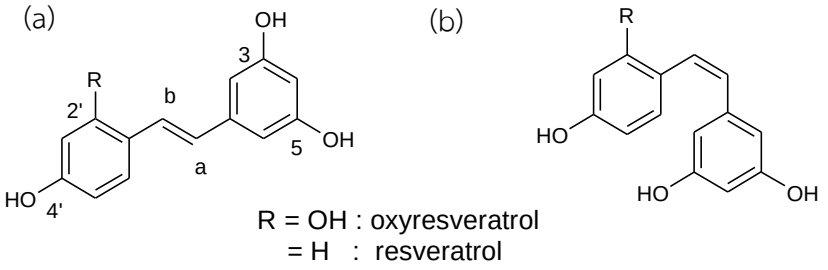

Figure A-5 Structures of (a) *trans*- and (b) *cis*-isomer of OXY and RES.

Table A-1 1H NMR data for OXY and RES.

Position	δ_H (int.,mult., *J* in Hz)			
	trans-OXY	*cis*-OXY	*trans*-RES	*cis*-RES
1	-	-	-	-
2,6	6.52 (2H, *d*, 2.0)	6.31 (2H, s)	6.53 (2H, d, 1.88)	6.28 (2H, d, 1.8)
3	-	-	-	-
4	6.24 (1H, *t*, 2.0)	6.28 (1H, *s*)	6.26 (1H, *t*, 1.8)	6.23 (1H, *t*, 2.2)
5	-	-	-	-
a	6.89 (1H, *d*, 16.4)	6.55 (1H, *d*, 8.3)	6.88 (1H, *d*, 16.4)	6.33 (1H, *d*, 12.2)
b	7.33 (1H, *d*, 16.4)	7.02 (1H, *d*, 8.8)	7.02 (1H, *d*, 16.4)	6.43 (1H, *d*, 12.8)
1'	-	-	-	-
2'	-	-	7.42 (2H, *d*, 8.4)	7.14 (2H, *d*, 8.3)
3'	6.44 (1H, *d*, 1.6)	6.39 (1H, *d*, 8.3)	6.84 (2H, *d*, 8.5)	6.70 (2H, *d*, 8.3)
4'	-	-	-	-
5'	6.39 (1H, *dd*, 8.0, 1.8)	6.18 (1H, *s*)	6.84 (2H, *d*, 8.5)	6.70 (2H, *d*, 8.3)
6'	7.41 (1H, *d*, 8.4)	6.16 (1H,*s*)	7.42 (2H, *d*, 8.4)	7.14 2H, *d*, 8.3)

APPENDIX B

Stability toward UV-A radiation

Stability toward UV-A radiation of *trans*-OXY and *trans*-RES.

The relative % of *trans-cis* oxyresveratrol (and resveratrol) was calculated with the following equation:

$$\%\text{Mole fraction } of trans - \text{isomer} = \frac{\text{PA}_{trans}}{\text{PA}_{cis} + \text{PA}_{trans}} \times 100$$

$$\%\text{Mole fraction } of cis - \text{isomer} = \frac{\text{PA}_{cis}}{\text{PA}_{cis} + \text{PA}_{trans}} \times 100$$

1. Oxyresveratrol

Table B-1 % Mole fraction of *cis* and *trans*-OXY at various irradiated time (1st replicated).

1st replicated	PA		% Mole fraction	
Time (min.)	*Trans* isomer	*Cis* isomer	*Trans* isomer	*Cis* isomer
0	1.00	0.00	100.00	0.00
5	1.00	0.38	72.67	27.33
10	1.00	0.68	59.52	40.48
20	1.00	2.22	31.03	68.97
30	1.00	5.47	15.46	84.54
40	1.00	6.60	13.15	86.85
50	1.00	6.62	13.12	86.88
60	1.00	6.82	12.80	87.20
80	1.00	6.77	12.88	87.13

Table B-2 % Mole fraction of *cis* and *trans*-OXY at various irradiated time (2nd replicated).

2nd replicated	PA		% Mole fraction	
Time (min.)	*Trans* isomer	*Cis* isomer	*Trans* isomer	*Cis* isomer
0	1.00	0.00	100.00	0.00
5	1.00	0.26	79.37	20.63
10	1.00	0.70	58.75	41.25
20	1.00	1.97	33.64	66.36
30	1.00	4.16	19.36	80.64
40	1.00	6.94	12.60	87.40
50	1.00	7.85	11.31	88.69
60	1.00	7.82	11.34	88.66
80	1.00	8.47	10.56	89.44

Table B-3 % Mole fraction of *cis* and *trans*-OXY at various irradiated time (3rd replicated).

3rd replicated	PA		% Mole fraction	
Time (min.)	*Trans* isomer	*Cis* isomer	*Trans* isomer	*Cis* isomer
0	1.00	0.00	100.00	0.00
5	1.00	0.25	80.16	19.84
10	1.00	0.75	56.98	43.02
20	1.00	2.00	33.35	66.65
30	1.00	5.02	16.61	83.39
40	1.00	5.45	15.51	84.49
50	1.00	6.15	13.99	86.01
60	1.00	6.38	13.56	86.44
80	1.00	6.76	12.98	87.02

Table B-4 % Mole fraction of *cis* and *trans*-OXY at various irradiated time.

Time (min.)	% Mole fraction of *trans*-OXY					% Mole fraction of *cis*-OXY				
	1st replicated	2nd replicated	3rd replicated	Aver.	SD	1st replicated	2nd replicated	3rd replicated	Aver.	SD
0	100.00	100.00	100.00	100.00	0.00	0.00	0.00	0.00	0.00	0.00
5	72.67	79.37	80.16	77.40	4.11	27.33	20.63	19.84	22.60	4.11
10	59.52	58.75	56.98	58.42	1.30	40.48	41.25	43.02	41.58	1.30
20	31.03	33.64	33.35	32.67	1.43	68.97	66.36	66.65	67.33	1.43
30	15.46	19.36	16.61	17.14	2.01	84.54	80.64	83.39	82.86	2.01
40	13.15	12.60	15.51	13.75	1.55	86.85	87.40	84.49	86.25	1.55
50	13.12	11.31	13.99	12.81	1.37	86.88	88.69	86.01	87.19	1.37
60	12.80	11.34	13.56	12.57	1.12	87.20	88.66	86.44	87.43	1.12
80	12.88	10.56	12.98	12.14	1.37	87.13	89.44	87.02	87.86	1.37

2 Resveratrol

Table B-5 % Mole fraction of *cis* and *trans*-RES at various irradiated time (1st replicated).

1st replicated	PA		% Mole fraction	
Time (min.)	*Trans* isomer	*Cis* isomer	*Trans* isomer	*Cis* isomer
0	1.00	0.00	100.00	0.00
5	1.00	0.34	74.57	25.43
10	1.00	0.44	69.49	30.51
20	1.00	0.87	53.50	46.50
30	1.00	1.66	37.64	62.36
40	1.00	2.73	26.80	73.20
50	1.00	3.83	20.70	79.30
60	1.00	5.72	14.88	85.12
80	1.00	7.13	12.30	87.70

Table B-6 % Mole fraction of *cis* and *trans*-RES at various irradiated time (2nd replicated).

2nd replicated	PA		% Mole fraction	
Time (min.)	*Trans* isomer	*Cis* isomer	*Trans* isomer	*Cis* isomer
0	1.00	0.00	100.00	0.00
5	1.00	0.20	83.61	16.39
10	1.00	0.32	75.76	24.24
20	1.00	0.81	55.34	44.66
30	1.00	1.73	36.66	63.34
40	1.00	2.19	31.38	68.62
50	1.00	3.54	22.03	77.97
60	1.00	4.36	18.67	81.33
80	1.00	4.20	19.22	80.78

Table B-7 % Mole fraction of *cis* and *trans*-RES at various irradiated time (3rd replicated).

3rd replicated	PA		% Mole fraction	
Time (min.)	*Trans* isomer	*Cis* isomer	*Trans* isomer	*Cis* isomer
0	1.00	0.00	100.00	0.00
5	1.00	0.27	78.51	21.49
10	1.00	0.36	73.40	26.61
20	1.00	0.80	55.46	44.54
30	1.00	1.53	39.58	60.42
40	1.00	2.50	28.56	71.44
50	1.00	3.35	23.00	77.00
60	1.00	4.60	17.86	82.14
80	1.00	5.31	15.86	84.14

Table B-8 % Mole fraction of *cis* and *trans*-RES at various irradiated time.

Time (min.)	% Mole fraction of *trans*-RES					% Mole fraction of *cis*-RES				
	1st replicated	2nd replicated	3rd replicated	Aver.	SD	1st replicated	2nd replicated	3rd replicated	Aver.	SD
0	100.00	100.00	100.00	100.00	0.00	0.00	0.00	0.00	0.00	0.00
5	74.57	83.61	78.51	78.90	4.53	25.43	16.39	21.49	21.10	4.53
10	69.49	75.76	73.40	72.88	3.16	30.51	24.24	26.61	27.12	3.16
20	53.50	55.34	55.46	54.77	1.10	46.50	44.66	44.54	45.23	1.10
30	37.64	36.66	39.58	37.96	1.49	62.36	63.34	60.42	62.04	1.49
40	26.80	31.38	28.56	28.91	2.31	73.20	68.62	71.44	71.09	2.31
50	20.70	22.03	23.00	21.91	1.15	79.30	77.97	77.00	78.09	1.15
60	14.88	18.67	17.86	17.14	2.00	85.12	81.33	82.14	82.86	2.00
80	12.30	19.22	15.86	15.79	3.46	87.70	80.78	84.14	84.21	3.46

APPENDIX C

Stability toward fluorescent light

Stability toward fluorescent light of *cis*-oxyresveratrol and *cis*-resveratrol.

1. ***Cis*-oxyresveratrol**

Table C-1 %Mole fraction of *cis* –OXY which was exposed to fluorescent light and protected from fluorescent light (1st replicated).

1st replicated	Exposed to fluorescent light				Protected from fluorescent light			
	PA		*Cis* isomer		PA		*Cis* isomer	
Days	*Cis* isomer	*Trans* isomer	% Mole fraction of *cis* isomer	%Normalized	*Cis* isomer	*Trans* isomer	% Mole fraction of *cis* isomer	%Normalized
0	3.654	1.000	78.51	100.00	3.654	1.000	78.51	78.51
1	0.507	1.000	33.64	42.85	0.359	1.000	26.41	33.64
2	0.138	1.000	12.13	15.45	0.105	1.000	9.52	12.13
3	0.067	1.000	6.28	8.00	0.052	1.000	4.93	6.28
4	0.060	1.000	5.28	7.23	0.052	1.000	4.93	6.28
5	0.044	1.000	4.22	5.38	0.034	1.000	3.32	4.22
6	0.033	1.000	3.22	4.10	0.026	1.000	2.53	3.22

Table C-2 %Mole fraction of *cis* –OXY which was exposed to fluorescent light and protected from fluorescent light (2nd replicated).

2nd replicated	Exposed to fluorescent light				Protected from fluorescent light			
	PA		Cis isomer		PA		Cis isomer	
Days	Cis isomer	Trans isomer	% Mole fraction of cis isomer	%Normalized	Cis isomer	Trans isomer	% Mole fraction of cis isomer	%Normalized
0	0.777	1.000	43.73	100.00	0.777	1.000	43.73	100.00
1	0.243	1.000	19.53	44.66	0.222	1.000	18.16	41.54
2	0.068	1.000	6.34	14.50	0.215	1.000	17.68	40.43
3	0.036	1.000	3.44	7.87	0.082	1.000	7.56	17.28
4	0.036	1.000	3.50	8.00	0.051	1.000	4.83	11.05
5	0.027	1.000	2.60	5.94	0.046	1.000	4.36	9.98
6	0.013	1.000	1.31	3.00	0.038	1.000	3.64	8.33

Table C-3 %Mole fraction of *cis*–OXY which was exposed to fluorescent light and protected from fluorescent light (3rd replicated).

3rd replicated	Exposed to fluorescent light				Protected from fluorescent light			
	PA		Cis isomer		PA		Cis isomer	
Days	Cis isomer	Trans isomer	% Mole fraction of cis isomer	%Normalized	Cis isomer	Trans isomer	% Mole fraction of cis isomer	%Normalized
0	1.572	1.000	61.12	100.00	1.572	1.000	61.12	100.00
1	0.362	1.000	26.59	43.75	0.287	1.000	22.29	35.54
2	0.102	1.000	9.23	14.97	0.157	1.000	13.60	21.54
3	0.099	1.000	9.00	9.00	0.099	1.000	9.00	11.51
4	0.048	1.000	4.59	7.61	0.051	1.000	4.88	7.95
5	0.035	1.000	3.41	5.66	0.040	1.000	3.84	6.23
6	0.023	1.000	2.26	3.55	0.032	1.000	3.08	5.78

Table C-4 %Mole fraction of *cis*–OXY which was exposed to fluorescent light and protected from fluorescent light.

Days	Exposed to fluorescent light					Protected from fluorescent light				
	%Normalized of cis isomer					%Normalized of cis isomer				
	1st replicated	2nd replicated	3rd replicated	Average	SD	1st replicated	2nd replicated	3rd replicated	Average	SD
0	100.00	100.00	100.00	100.00	0.00	100.00	100.00	100.00	100.00	0.00
1	42.85	44.66	43.75	43.75	0.90	42.85	41.54	35.54	39.98	3.90
2	15.45	14.50	14.97	14.97	0.47	15.45	40.43	21.54	25.81	13.02
3	8.00	7.87	9.00	8.29	0.62	8.00	17.28	11.51	12.26	4.69
4	7.23	8.00	7.61	7.61	0.38	8.00	11.05	7.95	9.00	1.78
5	5.38	5.94	5.66	5.66	0.28	5.38	9.98	6.23	7.20	2.45
6	4.10	3.00	3.55	3.55	0.55	4.10	8.33	5.78	6.07	2.13

Table C-5 %Mole fraction of *cis* –RES which was exposed to fluorescent light and protected from fluorescent light (1st replicated).

1st replicated	Exposed to fluorescent light				Protected from fluorescent light			
	PA		Cis isomer		PA		Cis isomer	
Days	Cis isomer	Trans isomer	% Mole fraction of cis isomer	%Normalized	Cis isomer	Trans isomer	% Mole fraction of cis isomer	%Normalized
0	1.067	1.000	51.62	100.00	1.067	1.000	51.62	100.00
1	0.548	1.000	35.40	68.58	0.591	1.000	37.15	71.96
2	0.468	1.000	31.88	61.76	0.527	1.000	34.51	66.86
3	0.465	1.000	31.74	61.49	0.525	1.000	34.42	66.68
4	0.336	1.000	25.15	48.72	0.515	1.000	33.99	65.85
5	0.245	1.000	19.68	38.12	0.497	1.000	33.20	64.31
6	0.103	1.000	9.34	18.09	0.432	1.000	30.16	58.43
7	0.081	1.000	7.49	14.52	0.300	1.000	23.07	44.70

Table C-6 %Mole fraction of *cis* –RES which was exposed to fluorescent light and protected from fluorescent light (2nd replicated).

2nd replicated	Exposed to fluorescent light				Protected from fluorescent light			
	PA		Cis isomer		PA		Cis isomer	
Days	Cis isomer	Trans isomer	% Mole fraction of cis isomer	%Normalized	Cis isomer	Trans isomer	% Mole fraction of cis isomer	%Normalized
0	2.450	1.000	71.01	100.00	0.94	1.00	48.53	100.00
1	1.869	1.000	65.14	91.75	0.814	1.000	44.87	92.46
2	1.640	1.000	62.12	87.49	0.704	1.000	41.31	85.13
3	0.609	1.000	37.85	53.30	0.737	1.000	42.43	87.42
4	0.427	1.000	29.92	42.14	0.491	1.000	32.93	67.85
5	0.215	1.000	17.70	24.92	0.394	1.000	28.26	58.24
6	0.282	1.000	22.00	30.98	0.368	1.000	26.90	55.43
7	0.176	1.000	14.97	21.08	0.281	1.000	21.94	45.20

Table C-7 %Mole fraction of *cis* –RES which was exposed to fluorescent light and protected from fluorescent light (3rd replicated).

3rd replicated	Exposed to fluorescent light				Protected from fluorescent light			
	PA		Cis isomer		PA		Cis isomer	
Days	Cis isomer	Trans isomer	% Mole fraction of cis isomer	%Normalized	Cis isomer	Trans isomer	% Mole fraction of cis isomer	%Normalized
0	1.758	1.000	63.74	100.00	1.003	1.000	50.08	100.00
1	1.209	1.000	54.72	85.85	0.695	1.000	41.01	82.21
2	1.054	1.000	51.31	80.50	0.611	1.000	37.91	75.99
3	0.537	1.000	34.94	54.81	0.625	1.000	38.47	77.14
4	0.382	1.000	27.61	43.32	0.515	1.000	33.98	67.85
5	0.230	1.000	18.70	29.34	0.444	1.000	30.73	61.28
6	0.193	1.000	16.14	25.32	0.375	1.000	27.26	54.43
7	0.129	1.000	11.39	17.86	0.293	1.000	22.63	45.20

Table C-8 %Mole fraction of *cis* –RES which was exposed to fluorescent light and protected from fluorescent light.

Days	Exposed to fluorescent light					Protected from fluorescent light				
	%Normalized of cis isomer					%Normalized of cis isomer				
	1st replicated	2nd replicated	3rd replicated	Average	SD	1st replicated	2nd replicated	3rd replicated	Average	SD
0	100.00	100.00	100.00	100.00	0.00	100.00	100.00	100.00	100.00	0.00
1	68.58	91.75	85.85	82.06	12.04	71.96	92.46	82.21	82.21	10.25
2	61.76	87.49	80.50	76.58	13.30	66.86	85.13	75.99	75.99	9.13
3	61.49	53.30	54.81	56.53	4.36	66.68	87.42	77.14	77.08	10.37
4	48.72	42.14	43.32	44.73	3.51	65.85	67.85	67.85	67.18	1.16
5	38.12	24.92	29.34	30.79	6.72	64.31	58.24	61.28	61.28	3.04
6	18.09	30.98	25.32	24.80	6.46	58.43	55.43	54.43	56.10	2.08
7	14.52	21.08	17.86	17.82	3.28	44.70	45.20	45.20	45.03	0.29

APPENDIX D

Stability toward Temperature

Stability toward Temperature

1. *Cis*-oxyresveratrol

Table D-1 % Mole fraction of *cis* OXY at 4 ºC, room temperature and 50 ºC (1st replicated). *N/A : not applicable*

1st replicated	4 ºC				Room temperature				50 ºC			
	PA		Cis isomer		PA		Cis isomer		PA		Cis isomer	
Time	*Cis* isomer	*Trans* isomer	% Mole fraction of cis isomer	%Normalized	*Cis* isomer	*Trans* isomer	% Mole fraction of cis isomer	%Normalized	*Cis* isomer	*Trans* isomer	% Mole fraction of cis isomer	%Normalized
0 day	0.777	1.000	43.73	100.00	3.654	1.000	78.51	100.00	2.807	1.000	73.73	100.00
1 h	N/A	N/A	N/A	N/A	N/A	N/A	N/A	N/A	1.434	1.000	58.92	79.90
2 h	N/A	N/A	N/A	N/A	N/A	N/A	N/A	N/A	0.976	1.000	49.40	67.00
3 h	N/A	N/A	N/A	N/A	N/A	N/A	N/A	N/A	0.517	1.000	34.08	46.22
4 h	N/A	N/A	N/A	N/A	N/A	N/A	N/A	N/A	0.456	1.000	31.32	42.48
5 h	N/A	N/A	N/A	N/A	N/A	N/A	N/A	N/A	0.367	1.000	26.85	36.41
6 h	N/A	N/A	N/A	N/A	N/A	N/A	N/A	N/A	0.185	1.000	15.61	21.17
1day	N/A	N/A	N/A	N/A	0.484	1.000	32.61	41.54	0.044	1.000	4.25	5.77
2 days	0.407	1.000	28.93	66.17	0.465	1.000	31.74	40.43	N/A	N/A	N/A	N/A
3 days	0.311	1.000	23.73	54.27	0.157	1.000	13.57	17.28	N/A	N/A	N/A	N/A
4 days	0.254	1.000	20.24	46.30	0.095	1.000	8.68	11.05	N/A	N/A	N/A	N/A
5 days	N/A	N/A	N/A	N/A	0.085	1.000	7.83	9.98	N/A	N/A	N/A	N/A
6 days	0.213	1.000	17.59	40.22	0.070	1.000	6.54	8.33	N/A	N/A	N/A	N/A
7 days	N/A	N/A	N/A	N/A	N/A	N/A	N/A	N/A	N/A	N/A	N/A	N/A
8 days	N/A	N/A	N/A	N/A	N/A	N/A	N/A	N/A	N/A	N/A	N/A	N/A
10 days	0.152	1.000	13.23	30.26	N/A	N/A	N/A	N/A	N/A	N/A	N/A	N/A
15 days	0.063	1.000	5.88	13.45	N/A	N/A	N/A	N/A	N/A	N/A	N/A	N/A
20 days	0.048	1.000	4.56	10.42	N/A	N/A	N/A	N/A	N/A	N/A	N/A	N/A

Ta Table D-2 % Mole fraction of *cis* OXY at 4 °C, room temperature and 50 °C (2nd replicated). *N/A : not applicable*

2nd replicated	4 °C				Room temperature				50 °C			
	PA		*Cis* isomer		PA		*Cis* isomer		PA		*Cis* isomer	
Time	*Cis* isomer	*Trans* isomer	% Mole fraction of cis isomer	%Normalized	*Cis* isomer	*Trans* isomer	% Mole fraction of cis isomer	%Normalized	*Cis* isomer	*Trans* isomer	% Mole fraction of cis isomer	%Normalized
0 day	1.572	1.000	61.12	100.00	1.572	1.000	61.12	100.00	1.798	1.000	64.26	100.00
1 h	N/A	N/A	N/A	N/A	N/A	N/A	N/A	N/A	1.014	1.000	50.34	78.34
2 h	N/A	N/A	N/A	N/A	N/A	N/A	N/A	N/A	0.670	1.000	40.11	62.42
3 h	N/A	N/A	N/A	N/A	N/A	N/A	N/A	N/A	0.422	1.000	29.67	46.16
4 h	N/A	N/A	N/A	N/A	N/A	N/A	N/A	N/A	0.369	1.000	26.97	41.97
5 h	N/A	N/A	N/A	N/A	N/A	N/A	N/A	N/A	0.264	1.000	20.90	32.52
6 h	N/A	N/A	N/A	N/A	N/A	N/A	N/A	N/A	0.170	1.000	14.54	22.63
1day	N/A	N/A	N/A	N/A	0.308	1.000	23.56	38.54	0.031	1.000	3.03	4.71
2 days	0.672	1.000	40.20	65.78	0.234	1.000	18.94	30.99	N/A	N/A	N/A	N/A
3 days	0.490	1.000	32.86	53.77	0.096	1.000	8.80	14.40	N/A	N/A	N/A	N/A
4 days	0.378	1.000	27.44	44.90	0.062	1.000	5.81	9.50	N/A	N/A	N/A	N/A
5 days	N/A	N/A	N/A	N/A	0.052	1.000	4.95	8.10	N/A	N/A	N/A	N/A
6 days	0.269	1.000	21.22	34.72	0.054	1.000	5.09	8.33	N/A	N/A	N/A	N/A
7 days	N/A	N/A	N/A	N/A	N/A	N/A	N/A	N/A	N/A	N/A	N/A	N/A
8 days	N/A	N/A	N/A	N/A	N/A	N/A	N/A	N/A	N/A	N/A	N/A	N/A
10 days	0.129	1.000	11.42	18.69	N/A	N/A	N/A	N/A	N/A	N/A	N/A	N/A
15 days	0.070	1.000	6.53	10.68	N/A	N/A	N/A	N/A	N/A	N/A	N/A	N/A
20 days	0.037	1.000	3.54	5.80	N/A	N/A	N/A	N/A	N/A	N/A	N/A	N/A

Table D-3 % Mole fraction of *cis* OXY at 4 °C, room temperature and 50 °C (3rd replicated). *N/A : not applicable*

3rd replicated	4 °C				Room temperature				50 °C			
	PA		*Cis* isomer		PA		*Cis* isomer		PA		*Cis* isomer	
Time	*Cis* isomer	*Trans* isomer	% Mole fraction of cis isomer	%Normalized	*Cis* isomer	*Trans* isomer	% Mole fraction of cis isomer	%Normalized	*Cis* isomer	*Trans* isomer	% Mole fraction of cis isomer	%Normalized
0 day	3.654	1.000	78.51	100.00	0.777	1.000	43.73	100.00	1.212	1.000	54.79	100.00
1 h	N/A	N/A	N/A	N/A	N/A	N/A	N/A	N/A	0.726	1.000	42.06	76.77
2 h	N/A	N/A	N/A	N/A	N/A	N/A	N/A	N/A	0.464	1.000	31.69	57.84
3 h	N/A	N/A	N/A	N/A	N/A	N/A	N/A	N/A	0.338	1.000	25.26	46.10
4 h	N/A	N/A	N/A	N/A	N/A	N/A	N/A	N/A	0.294	1.000	22.72	41.47
5 h	N/A	N/A	N/A	N/A	N/A	N/A	N/A	N/A	0.186	1.000	15.68	28.62
6 h	N/A	N/A	N/A	N/A	N/A	N/A	N/A	N/A	0.152	1.000	13.19	24.08
1day	N/A	N/A	N/A	N/A	0.184	1.000	15.54	35.54	0.028	1.000	2.74	4.27
2 days	1.015	1.000	50.38	64.17	0.104	1.000	9.42	21.54	N/A	N/A	N/A	N/A
3 days	0.696	1.000	41.04	52.27	0.053	1.000	5.03	11.51	N/A	N/A	N/A	N/A
4 days	0.552	1.000	35.57	45.30	0.036	1.000	3.47	7.95	N/A	N/A	N/A	N/A
5 days	N/A	N/A	N/A	N/A	0.028	1.000	2.72	6.23	N/A	N/A	N/A	N/A
6 days	0.560	1.000	35.90	45.72	0.023	1.000	2.29	5.23	N/A	N/A	N/A	N/A
7 days	N/A	N/A	N/A	N/A	N/A	N/A	N/A	N/A	N/A	N/A	N/A	N/A
8 days	N/A	N/A	N/A	N/A	N/A	N/A	N/A	N/A	N/A	N/A	N/A	N/A
10 days	0.489	1.000	32.84	41.83	N/A	N/A	N/A	N/A	N/A	N/A	N/A	N/A
15 days	0.146	1.000	12.74	16.23	N/A	N/A	N/A	N/A	N/A	N/A	N/A	N/A
20 days	0.134	1.000	11.82	15.05	N/A	N/A	N/A	N/A	N/A	N/A	N/A	N/A

Table D-4 % Mole fraction of *cis* OXY at 4 ℃, room temperature and 50 ℃. *N/A : not applicable*

Time	4 ℃					Room temperature					50 ℃				
	1st replicated	2nd replicated	3rd replicated	Aver.	SD	1st replicated	2nd replicated	3rd replicated	Aver.	SD	1st replicated	2nd replicated	3rd replicated	Aver.	SD
0 day	100.00	100.00	100.00	100.00	0.00	100.00	100.00	100.00	100.00	0.00	100.00	100.00	100.00	100.00	0.00
1 h	N/A	N/A	N/A	N/A	N/A	N/A	N/A	N/A	N/A	N/A	79.90	78.34	76.77	78.34	1.57
2 h	N/A	N/A	N/A	N/A	N/A	N/A	N/A	N/A	N/A	N/A	67.00	62.42	57.84	62.42	4.58
3 h	N/A	N/A	N/A	N/A	N/A	N/A	N/A	N/A	N/A	N/A	46.22	46.16	46.10	46.16	0.06
4 h	N/A	N/A	N/A	N/A	N/A	N/A	N/A	N/A	N/A	N/A	42.48	41.97	41.47	41.97	0.50
5 h	N/A	N/A	N/A	N/A	N/A	N/A	N/A	N/A	N/A	N/A	36.41	32.52	28.62	32.52	3.89
6 h	N/A	N/A	N/A	N/A	N/A	N/A	N/A	N/A	N/A	N/A	21.17	22.63	24.08	22.63	1.45
1day	N/A	N/A	N/A	N/A	N/A	41.54	38.54	35.54	38.54	3.00	5.77	4.27	5.02	5.02	0.75
2 days	66.17	65.78	65.97	65.97	0.19	40.43	30.99	21.54	30.99	9.44	N/A	N/A	N/A	N/A	N/A
3 days	54.27	53.77	52.27	53.44	1.04	17.28	14.40	11.51	14.40	2.89	N/A	N/A	N/A	N/A	N/A
4 days	46.30	44.90	45.60	45.60	0.70	11.05	9.50	7.95	9.50	1.55	N/A	N/A	N/A	N/A	N/A
5 days	N/A	N/A	N/A	N/A	N/A	9.98	8.10	6.23	8.10	1.87	N/A	N/A	N/A	N/A	N/A
6 days	40.22	34.72	45.72	40.22	5.50	8.33	8.33	5.23	7.30	1.79	N/A	N/A	N/A	N/A	N/A
7 days	N/A	N/A	N/A	N/A	N/A	N/A	N/A	N/A	N/A	N/A	N/A	N/A	N/A	N/A	N/A
8 days	N/A	N/A	N/A	N/A	N/A	N/A	N/A	N/A	N/A	N/A	N/A	N/A	N/A	N/A	N/A
10 days	30.26	18.69	41.83	30.26	11.57	N/A	N/A	N/A	N/A	N/A	N/A	N/A	N/A	N/A	N/A
15 days	13.45	10.68	16.23	13.45	2.77	N/A	N/A	N/A	N/A	N/A	N/A	N/A	N/A	N/A	N/A
20 days	10.42	5.80	15.05	10.42	4.63	N/A	N/A	N/A	N/A	N/A	N/A	N/A	N/A	N/A	N/A

Table D-5 % Mole fraction of *cis* RES at 4 °C, room temperature and 50 °C (1st replicated). *N/A : not applicable*

1st replicated	4 °C				Room temperature				50 °C			
	PA		*Cis* isomer		PA		*Cis* isomer		PA		*Cis* isomer	
Time	*Cis* isomer	*Trans* isomer	% Mole fraction of cis isomer	%Normalized	*Cis* isomer	*Trans* isomer	% Mole fraction of cis isomer	%Normalized	*Cis* isomer	*Trans* isomer	% Mole fraction of cis isomer	%Normalized
0 day	2.449	1.000	71.01	100.00	1.003	1.000	50.08	100.00	4.746	1.000	82.60	100.00
1 h	N/A	N/A	N/A	N/A	N/A	N/A	N/A	N/A	4.209	1.000	80.80	97.83
2 h	N/A	N/A	N/A	N/A	N/A	N/A	N/A	N/A	4.376	1.000	81.40	98.55
3 h	N/A	N/A	N/A	N/A	N/A	N/A	N/A	N/A	4.172	1.000	80.67	97.66
4 h	N/A	N/A	N/A	N/A	N/A	N/A	N/A	N/A	4.433	1.000	81.59	98.79
5 h	N/A	N/A	N/A	N/A	N/A	N/A	N/A	N/A	3.864	1.000	79.44	96.18
6 h	N/A	N/A	N/A	N/A	N/A	N/A	N/A	N/A	4.069	1.000	80.27	97.19
1day	N/A	N/A	N/A	N/A	0.700	1.000	41.17	82.21	3.870	1.000	79.47	96.21
2 days	2.247	1.000	69.20	97.46	0.614	1.000	38.05	75.99	N/A	N/A	N/A	N/A
3 days	N/A	N/A	N/A	N/A	0.629	1.000	38.63	77.14	N/A	N/A	N/A	N/A
4 days	1.994	1.000	66.60	93.79	0.515	1.000	33.98	67.85	N/A	N/A	N/A	N/A
5 days	N/A	N/A	N/A	N/A	0.443	1.000	30.68	61.28	N/A	N/A	N/A	N/A
6 days	2.257	1.000	69.30	97.59	0.375	1.000	27.26	54.43	N/A	N/A	N/A	N/A
7 days	N/A	N/A	N/A	N/A	0.293	1.000	22.63	45.20	N/A	N/A	N/A	N/A
8 days	2.393	1.000	70.53	99.33	N/A	N/A	N/A	N/A	N/A	N/A	N/A	N/A
10 days	2.309	1.000	69.78	98.27	N/A	N/A	N/A	N/A	N/A	N/A	N/A	N/A
15 days	2.103	1.000	67.77	95.44	N/A	N/A	N/A	N/A	N/A	N/A	N/A	N/A
20 days	2.363	1.000	70.26	98.96	N/A	N/A	N/A	N/A	N/A	N/A	N/A	N/A

Table D-6 % Mole fraction of *cis* RES at 4 °C, room temperature and 50 °C (2nd replicated). *N/A : not applicable*

2nd replicated	4 °C				Room temperature				50 °C			
	PA		*Cis* isomer		PA		*Cis* isomer		PA		*Cis* isomer	
Time	*Cis* isomer	*Trans* isomer	% Mole fraction of cis isomer	%Normalized	*Cis* isomer	*Trans* isomer	% Mole fraction of cis isomer	%Normalized	*Cis* isomer	*Trans* isomer	% Mole fraction of cis isomer	%Normalized
0 day	1.067	1.000	51.62	100.00	0.943	1.000	48.53	100.00	2.828	1.000	73.88	100.00
1 h	N/A	N/A	N/A	N/A	N/A	N/A	N/A	N/A	2.474	1.000	71.21	96.40
2 h	N/A	N/A	N/A	N/A	N/A	N/A	N/A	N/A	2.725	1.000	73.15	99.02
3 h	N/A	N/A	N/A	N/A	N/A	N/A	N/A	N/A	2.701	1.000	72.98	98.79
4 h	N/A	N/A	N/A	N/A	N/A	N/A	N/A	N/A	2.574	1.000	72.02	97.49
5 h	N/A	N/A	N/A	N/A	N/A	N/A	N/A	N/A	2.376	1.000	70.38	95.27
6 h	N/A	N/A	N/A	N/A	N/A	N/A	N/A	N/A	1.982	1.000	66.47	89.97
1day	N/A	N/A	N/A	N/A	0.814	1.000	44.87	92.46	1.547	1.000	60.74	82.22
2 days	1.060	1.000	51.45	99.67	0.704	1.000	41.31	85.13	N/A	N/A	N/A	N/A
3 days	N/A	N/A	N/A	N/A	0.737	1.000	42.43	87.42	N/A	N/A	N/A	N/A
4 days	0.968	1.000	49.19	95.29	0.491	1.000	32.93	67.85	N/A	N/A	N/A	N/A
5 days	N/A	N/A	N/A	N/A	0.394	1.000	28.26	58.24	N/A	N/A	N/A	N/A
6 days	0.975	1.000	49.36	95.61	0.359	1.000	26.42	54.43	N/A	N/A	N/A	N/A
7 days	N/A	N/A	N/A	N/A	0.281	1.000	21.94	45.20	N/A	N/A	N/A	N/A
8 days	0.936	1.000	48.36	93.68	N/A	N/A	N/A	N/A	N/A	N/A	N/A	N/A
10 days	0.952	1.000	48.77	94.48	N/A	N/A	N/A	N/A	N/A	N/A	N/A	N/A
15 days	1.021	1.000	50.52	97.87	N/A	N/A	N/A	N/A	N/A	N/A	N/A	N/A
20 days	0.947	1.000	48.65	94.24	N/A	N/A	N/A	N/A	N/A	N/A	N/A	N/A

Table D-7 % Mole fraction of *cis* RES at 4 °C, room temperature and 50 °C (3rd replicated). *N/A : not applicable*

3rd replicated	4 °C				Room temperature				50 °C			
	PA		*Cis* isomer		PA		*Cis* isomer		PA		*Cis* isomer	
Time	*Cis* isomer	*Trans* isomer	% Mole fraction of cis isomer	%Normalized	*Cis* isomer	*Trans* isomer	% Mole fraction of cis isomer	%Normalized	*Cis* isomer	*Trans* isomer	% Mole fraction of cis isomer	%Normalized
0 day	1.585	1.000	61.31	100.00	1.067	1.000	51.62	100.00	3.595	1.000	78.24	100.00
1 h	N/A	N/A	N/A	N/A	N/A	N/A	N/A	N/A	3.168	1.000	76.01	97.11
2 h	N/A	N/A	N/A	N/A	N/A	N/A	N/A	N/A	3.401	1.000	77.28	98.79
3 h	N/A	N/A	N/A	N/A	N/A	N/A	N/A	N/A	3.315	1.000	76.82	98.22
4 h	N/A	N/A	N/A	N/A	N/A	N/A	N/A	N/A	3.312	1.000	76.81	98.14
5 h	N/A	N/A	N/A	N/A	N/A	N/A	N/A	N/A	2.986	1.000	74.91	95.72
6 h	N/A	N/A	N/A	N/A	N/A	N/A	N/A	N/A	2.755	1.000	73.37	93.58
1day	N/A	N/A	N/A	N/A	0.865	1.000	46.39	71.96	2.345	1.000	70.10	89.21
2 days	1.521	1.000	60.33	98.56	0.813	1.000	44.84	66.86	N/A	N/A	N/A	N/A
3 days	N/A	N/A	N/A	N/A	0.822	1.000	45.13	66.57	N/A	N/A	N/A	N/A
4 days	1.375	1.000	57.90	96.80	0.748	1.000	42.80	67.85	N/A	N/A	N/A	N/A
5 days	N/A	N/A	N/A	N/A	0.699	1.000	41.15	64.31	N/A	N/A	N/A	N/A
6 days	1.459	1.000	59.33	93.64	0.651	1.000	39.44	54.43	N/A	N/A	N/A	N/A
7 days	N/A	N/A	N/A	N/A	0.591	1.000	37.13	43.43	N/A	N/A	N/A	N/A
8 days	1.466	1.000	59.44	88.04	N/A	N/A	N/A	N/A	N/A	N/A	N/A	N/A
10 days	1.455	1.000	59.27	90.68	N/A	N/A	N/A	N/A	N/A	N/A	N/A	N/A
15 days	1.543	1.000	60.67	98.96	N/A	N/A	N/A	N/A	N/A	N/A	N/A	N/A
20 days	1.308	1.000	56.68	92.44	N/A	N/A	N/A	N/A	N/A	N/A	N/A	N/A

Table D-8 % Mole fraction of *cis* RES at 4 °C, room temperature and 50 °C. *N/A : not applicable*

Time	4 °C					Room temperature					50 °C				
	1st replicated	2nd replicated	3rd replicated	Aver.	SD	1st replicated	2nd replicated	3rd replicated	Aver.	SD	1st replicated	2nd replicated	3rd replicated	Aver.	SD
0 day	100.00	100.00	100.00	100.00	0.00	100.00	100.00	100.00	100.00	0.00	100.00	100.00	100.00	100.00	0.00
1 h	N/A	N/A	N/A	N/A	N/A	N/A	N/A	N/A	N/A	N/A	97.83	96.40	97.11	97.11	0.72
2 h	N/A	N/A	N/A	N/A	N/A	N/A	N/A	N/A	N/A	N/A	98.55	99.02	98.79	98.79	0.24
3 h	N/A	N/A	N/A	N/A	N/A	N/A	N/A	N/A	N/A	N/A	97.66	98.79	98.22	98.22	0.56
4 h	N/A	N/A	N/A	N/A	N/A	N/A	N/A	N/A	N/A	N/A	98.79	97.49	98.14	98.14	0.65
5 h	N/A	N/A	N/A	N/A	N/A	N/A	N/A	N/A	N/A	N/A	96.18	95.27	95.72	95.72	0.46
6 h	N/A	N/A	N/A	N/A	N/A	N/A	N/A	N/A	N/A	N/A	97.19	89.97	93.58	93.58	3.61
1day	N/A	N/A	N/A	N/A	N/A	82.21	92.46	71.96	82.21	10.25	96.21	82.22	89.21	89.21	7.00
2 days	97.46	99.67	98.56	98.56	1.10	75.99	85.13	66.86	75.99	9.13	N/A	N/A	N/A	N/A	N/A
3 days	N/A	N/A	N/A	N/A	N/A	77.14	87.42	66.57	77.05	10.43	N/A	N/A	N/A	N/A	N/A
4 days	93.79	95.29	96.80	95.29	1.50	67.85	67.85	67.85	67.85	0.00	N/A	N/A	N/A	N/A	N/A
5 days	N/A	N/A	N/A	N/A	N/A	61.28	58.24	64.31	61.28	3.04	N/A	N/A	N/A	N/A	N/A
6 days	97.59	95.61	93.64	95.61	1.98	54.43	54.43	54.43	54.43	0.00	N/A	N/A	N/A	N/A	N/A
7 days	N/A	N/A	N/A	N/A	N/A	45.20	45.20	43.43	44.61	1.02	N/A	N/A	N/A	N/A	N/A
8 days	99.33	93.68	88.04	93.68	5.65	N/A	N/A	N/A	N/A	N/A	N/A	N/A	N/A	N/A	N/A
10 days	98.27	94.48	90.68	94.48	3.80	N/A	N/A	N/A	N/A	N/A	N/A	N/A	N/A	N/A	N/A
15 days	95.44	97.87	96.66	96.66	1.22	N/A	N/A	N/A	N/A	N/A	N/A	N/A	N/A	N/A	N/A
20 days	98.96	94.24	96.60	96.60	2.36	N/A	N/A	N/A	N/A	N/A	N/A	N/A	N/A	N/A	N/A

APPENDIX E

Encapsulation efficiency and loading capacity

Encapsulation efficiency (%EE) and loading capacity (%LC) of *trans*-OXY.

Table E-1 OXY concentration and its corresponding absorbance value at 328 nm in ethanol solution.

Concentration (ppm)	2	4	5	6	8	10
Absorbance at 328 nm	0.16350	0.30740	0.39364	0.45647	0.60320	0.73844

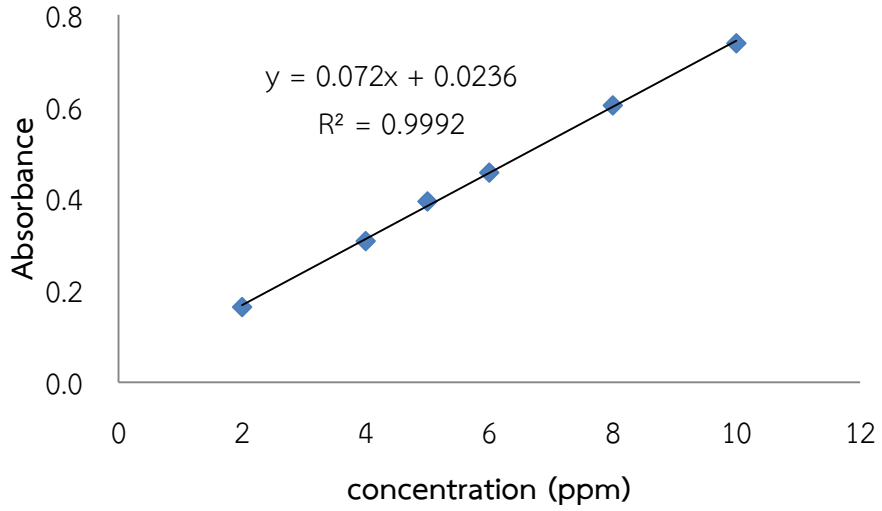

Figure E-1 calibration curve of *trans*-OXY in ethanol solution at 328 nm.

$$\%\mathrm{EE} = \frac{\text{Weight of encapsulated OXY in the particles}}{\text{Weight of OXY initially used}} \times 100$$

$$\%\mathrm{LC} = \frac{\text{Weight of encapsulated OXY in the particles}}{\text{Weight of the encapsulate OXY+polymer}} \times 100$$

Table E-2 %EE and %LC of *trans*-OXY loaded nanospheres

		Abs.	Conc. *trans*-OXY (ppm)	Dilution factor	Amount of *trans*-OXY (mg)	*Trans*-OXY used (mg)	Amount of EC (mg)	Amount of ME (mg)	%EE	%LC
Batch 1	1st replicated	0.4594	6.0531	100	12.1	20.0	40.0	0.0	60.5	23.2
	2nd replicated	0.4661	6.1463	100	12.3	20.0	40.0	0.0	61.5	23.5
	3rd replicated	0.4355	5.7212	100	11.4	20.0	40.0	0.0	57.2	22.2
								average	59.7±2.2	23.0±0.7
Batch2	1st replicated	0.5501	7.3131	100	14.6	30.0	30.0	0.0	48.8	32.8
	2nd replicated	0.5287	7.0147	100	14.0	30.0	30.0	0.0	46.8	31.9
	3rd replicated	0.5667	7.5434	100	15.1	30.0	30.0	0.0	50.3	33.5
								average	48.6±1.8	32.7±0.8
Batch 3	1st replicated	0.5917	7.8907	100	15.8	20.0	20.0	20.0	78.9	28.3
	2nd replicated	0.5519	7.3369	100	14.7	20.0	20.0	20.0	73.4	26.8
	3rd replicated	0.5689	7.5739	100	15.1	20.0	20.0	20.0	75.7	27.5
								average	76.0±2.8	27.5±0.7
Batch 4	1st replicated	0.6047	8.0714	100	16.1	30.0	15.0	15.0	53.8	35.0
	2nd replicated	0.6374	8.5250	100	17.1	30.0	15.0	15.0	56.8	36.2
	3rd replicated	0.6190	8.2700	100	16.5	30.0	15.0	15.0	55.1	35.5
								average	55.3±1.5	35.6±0.6

APPENDIX F

Calculation of %release

Calculation of %release

Table F-1 OXY concentration and its corresponding absorbance value at 328 nm in phosphate buffer solution pH 5.5.

Concentration (ppm)	2	4	6	8	10
Absorbance at 328 nm	0.15419	0.32469	0.47070	0.59166	0.75749

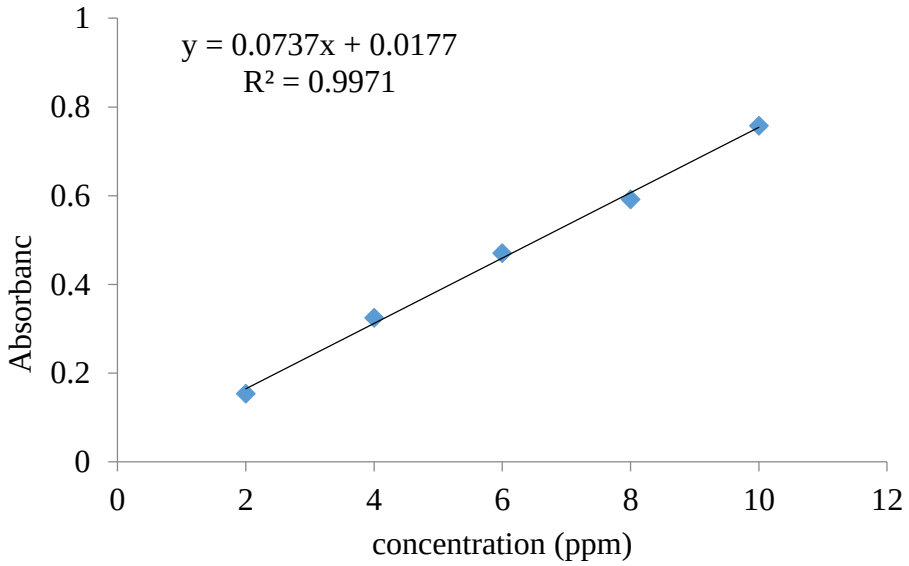

Figure F-1 Calibration curve of *trans*-OXY at 328 nm in phosphate buffer solution pH 5.5.

$$\%trans - \text{OXY released} = \frac{\text{Weight of encapsulated OXY in release medium}}{\text{Weight of encapsulated OXY}} \times 100$$

1. ***Trans*-OXY loaded nanospheres**

Table F-2 %Release of *trans*-OXY loaded nanospheres in phosphate buffer solution pH 5.5 (1st replicated).

Time (h)	Absorbance	Conc. *trans*-OXY (ppm)	Amount of *trans*-OXY (mg)	*Trans*-OXY initial used (mg)	% *Trans*-OXY released	% Relative released
0	0.0000	0.000	0.0	0.0	0.0	0.0
1	0.2146	2.672	1.3	10.0	13.4	31.8
2	0.3600	4.644	2.3	10.0	23.2	55.2
3	0.4376	5.697	2.8	10.0	28.5	67.7
4	0.4829	6.312	3.2	10.0	31.6	75.1
6	0.5800	7.629	3.8	10.0	38.1	90.7
7	0.6003	7.905	4.0	10.0	39.5	94.0
8	0.6512	8.596	4.3	10.0	43.0	102.2
24	0.6375	8.410	4.2	10.0	42.1	100.0

Table F-3 %Release of *trans*-OXY loaded nanospheres in phosphate buffer solution pH 5.5 (2nd replicated).

Time (h)	Absorbance	Conc. *trans*-OXY (ppm)	Amount of *trans*-OXY (mg)	*Trans*-OXY initial used (mg)	% *Trans*-OXY released	% relative released
0	0.0000	0.000	0.0	0.0	0.0	0.0
1	0.2330	2.922	1.5	10.0	14.6	25.9
2	0.3829	4.955	2.5	10.0	24.8	43.9
3	0.5186	6.796	3.4	10.0	34.0	60.3
4	0.6554	8.652	4.3	10.0	43.3	76.7
5	0.7951	10.549	5.3	10.0	52.7	93.5
6	0.8183	10.862	5.4	10.0	54.3	96.3
8	0.8593	11.419	5.7	10.0	57.1	101.3
24	0.8488	11.277	5.6	10.0	56.4	100.0

Table F-4 %Release of *trans*-OXY loaded nanospheres in phosphate buffer solution pH 5.5 (3rd replicated).

Time (h)	Absorbance	Conc. *trans*-OXY (ppm)	Amount of *trans*-OXY (mg)	*Trans*-OXY initial used (mg)	% *Trans*-OXY released	% relative released
0	0.0000	0.000	0.0	0.0	0.0	0.0
1	0.1997	2.469	1.2	10.0	12.3	23.1
2	0.3409	4.386	2.2	10.0	21.9	41.0
3	0.4620	6.028	3.0	10.0	30.1	56.4
4	0.6334	8.355	4.2	10.0	41.8	78.1
6	0.7986	10.595	5.3	10.0	53.0	99.0
7	0.8155	10.824	5.4	10.0	54.1	101.2
8	0.8017	10.638	5.3	10.0	53.2	99.4
24	0.8062	10.698	5.3	10.0	53.5	100.0

Table F-5 %%Release of *trans*-OXY loaded nanospheres in phosphate buffer solution pH 5.5.

trans-OXY	% relative released				
Time (h)	1st replicated	2nd replicated	3rd replicated	Average	SD
0	0.0	0.0	0.0	0.0	0.0
1	31.8	25.9	23.1	26.9	4.4
2	55.2	43.9	41.0	46.7	7.5
3	67.7	60.3	56.4	61.5	5.8
4	75.1	76.7	78.1	76.6	1.5
6	90.7	93.5	99.0	94.4	4.2
7	94.0	96.3	101.2	97.2	3.7
8	102.2	101.3	99.4	101.0	1.4
24	100.0	100.0	100.0	100.0	0.0

2. Free *trans*-OXY

Table F-6 %Release of free *trans*-OXY in phosphate buffer solution pH 5.5 (1st replicated).

Time (h)	Absorbance	Conc. *trans*-OXY (ppm)	Amount of *trans*-OXY (mg)	*Trans*-OXY initial used (mg)	% *Trans*-OXY released	% relative released
0	0.0000	0.000	0.0	0.0	0.0	0.0
1	0.26729	3.387	1.7	10.0	16.9	46.5
2	0.35366	4.558	2.3	10.0	22.8	62.5
3	0.45086	5.877	2.9	10.0	29.4	80.6
4	0.50833	6.657	3.3	10.0	33.3	91.3
6	0.52252	6.850	3.4	10.0	34.2	94.0
7	0.53983	7.085	3.5	10.0	35.4	97.2
8	0.53580	7.030	3.5	10.0	35.1	96.4
24	0.55490	7.289	3.6	10.0	36.4	100.0

Table F-7 %Release of free *trans*-OXY in phosphate buffer solution pH 5.5 (2nd replicated).

Time (h)	Absorbance	Conc. *trans*-OXY (ppm)	Amount of *trans*-OXY (mg)	*Trans*-OXY initial used (mg)	% *Trans*-OXY released	% relative released
0	0.0000	0.000	0.0	0.0	0.0	0.0
1	0.32724	4.200	2.1	10.0	21.0	42.1
2	0.56252	7.392	3.7	10.0	37.0	74.1
3	0.71727	9.492	4.7	10.0	47.5	95.2
4	0.80022	10.618	5.3	10.0	53.1	106.4
5	0.70469	9.321	4.7	10.0	46.6	93.4
6	0.78394	10.397	5.2	10.0	52.0	104.2
8	0.79724	10.577	5.3	10.0	52.9	106.0
24	0.75290	9.976	5.0	10.0	49.9	100.0

Table F-8 %Release of free *trans*-OXY in phosphate buffer solution pH 5.5 (3rd replicated)

Time (h)	Absorbance	Conc. *trans*-OXY (ppm)	Amount of *trans*-OXY (mg)	*Trans*-OXY initial used (mg)	% *Trans*-OXY released	% relative released
0	0.0000	0.000	0.0	0.0	0.0	0.0
1	0.31012	3.968	2.0	10.0	19.8	40.4
2	0.57699	7.589	3.8	10.0	37.9	77.3
3	0.72199	9.556	4.8	10.0	47.8	97.3
4	0.82004	10.887	5.4	10.0	54.4	110.9
6	0.77191	10.234	5.1	10.0	51.2	104.2
7	0.82052	10.893	5.4	10.0	54.5	110.9
8	0.81990	10.885	5.4	10.0	54.4	110.8
24	0.74144	9.820	4.9	10.0	49.1	100.0

Table F-9 %Release of free *trans*-OXY in phosphate buffer solution pH 5.5.

Trans-OXY loaded in nanospheres	% Relative released				
Time (h)	1st replicated	2nd replicated	3rd replicated	Average	SD
0	0.0	0.0	0.0	0.0	0.0
1	46.5	42.1	40.4	43.0	3.1
2	62.5	74.1	77.3	71.3	7.8
3	80.6	95.2	97.3	91.0	9.1
4	91.3	106.4	110.9	102.9	10.2
6	94.0	93.4	104.2	97.2	6.1
7	97.2	104.2	110.9	104.1	6.9
8	96.4	106.0	110.8	104.4	7.3
24	100.0	100.0	100.0	100.0	0.0

REFERENCES

[1] Maneechai, S., De-Eknamkul, W., Umehara, K., Noguchi, H., and Likhitwitayawuid, K. Flavonoid and stilbenoid production in callus cultures of Artocarpus lakoocha. Phytochemistry 81 (2012): 42-9.

[2] Likhitwitayawuid, K., Sornsute, A., Sritularak, B., and Ploypradith, P. Chemical transformations of oxyresveratrol (trans-2,4,3',5'-tetrahydroxystilbene) into a potent tyrosinase inhibitor and a strong cytotoxic agent. Bioorg Med Chem Lett 16(21) (2006): 5650-3.

[3] Weber, J.T., et al. Potential neuroprotective effects of oxyresveratrol against traumatic injury. Eur J Pharmacol 680(1-3) (2012): 55-62.

[4] Chuanasa, T., et al. Anti-herpes simplex virus (HSV-1) activity of oxyresveratrol derived from Thai medicinal plant: mechanism of action and therapeutic efficacy on cutaneous HSV-1 infection in mice. Antiviral Res 80(1) (2008): 62-70.

[5] Zaki, M.A., et al. Cytotoxicity and modulation of cancer-related signaling by (Z)- and (E)-3,4,3',5'-tetramethoxystilbene isolated from Eugenia rigida. J Nat Prod 76(4) (2013): 679-84.

[6] Mikulski, D., Gorniak, R., and Molski, M. A theoretical study of the structure-radical scavenging activity of trans-resveratrol analogues and cis-resveratrol in gas phase and water environment. Eur J Med Chem 45(3) (2010): 1015-27.

[7] Ruan, B.F., et al. Synthesis, biological evaluation and molecular docking studies of resveratrol derivatives possessing curcumin moiety as potent antitubulin agents. Bioorg Med Chem 20(2) (2012): 1113-21.

[8] Nedovic, V., Kalusevic, A., Manojlovic, V., Levic, S., and Bugarski, B. An overview of encapsulation technologies for food applications. Procedia Food Science 1 (2011): 1806-1815.

[9] Mak, W.C., et al. Drug delivery into the skin by degradable particles. Eur J Pharm Biopharm 79(1) (2011): 23-7.

[10] Suwannateep, N., Banlunara, W., Wanichwecharungruang, S.P., Chiablaem, K., Lirdprapamongkol, K., and Svasti, J. Mucoadhesive curcumin nanospheres:

biological activity, adhesion to stomach mucosa and release of curcumin into the circulation. J Control Release 151(2) (2011): 176-82.

[11] Likhitwitayawuid, K., Supudompol, B., Sritularak, B., Lipipun, V., Rapp, K., and Schinazi, R. Phenolics with Anti-HSV and Anti-HIV Activities from Artocarpus gomezianus., Mallotus pallidus., and Triphasia trifolia. Pharmaceutical biology 43(8) (2005): 651-657.

[12] Chao, J., Yu, M.S., Ho, Y.S., Wang, M., and Chang, R.C. Dietary oxyresveratrol prevents parkinsonian mimetic 6-hydroxydopamine neurotoxicity. Free Radic Biol Med 45(7) (2008): 1019-26.

[13] Lorenz, P., Roychowdhury, S., Engelmann, M., Wolf, G., and Horn, T.F.W. Oxyresveratrol and resveratrol are potent antioxidants and free radical scavengers: effect on nitrosative and oxidative stress derived from microglial cells. Nitric Oxide 9(2) (2003): 64-76.

[14] Shin, N.-H., et al. Oxyresveratrol as the Potent Inhibitor on Dopa Oxidase Activity of Mushroom Tyrosinase. Biochemical and Biophysical Research Communications 243(3) (1998): 801-803.

[15] Shimoni, N.J.Z.a.E. Overview of Microencapsulates for Use in Food Products or Processes and Methods to Make Them. Heart Vessels 19(1) (2004): 19-22.

[16] Murtaza, G. Ethyl cellulose microparticles: A review. Acta Poloniae Pharmaceutica - Drug Research 69(1) (2012): 11-22.

[17] Wang, W., Sun, L., Zhang, P., Song, J., and Liu, W. An anti-inflammatory cell-free collagen/resveratrol scaffold for repairing osteochondral defects in rabbits. Acta Biomater 10(12) (2014): 4983-95.

[18] Soppimath, K.S., Aminabhavi, T.M., Kulkarni, A.R., and Rudzinski, W.E. Biodegradable polymeric nanoparticles as drug delivery devices. in *Journal of Controlled Release*. 2001. 1–20.

[19] Blanco, D. and Alonso, M.a.J. Protein encapsulation and release from poly(lactide-co-glycolide) microspheres: effect of the protein and polymer properties and of the co-encapsulation of surfactants. European Journal of Pharmaceutics and Biopharmaceutics 45(3) (1998): 285-294.

[20] Rojas, J., Pinto-Alphandary, H., Leo, E., Pecquet, S., Couvreur, P., and Fattal, E. Optimization of the encapsulation and release of β -lactoglobulin entrapped poly(dl-lactide-co-glycolide) microspheres. Int J Pharm 183(1) (1999): 67-71.

[21] Luan, X., Skupin, M., Siepmann, J., and Bodmeier, R. Key parameters affecting the initial release (burst) and encapsulation efficiency of peptide-containing poly(lactide-co-glycolide) microparticles. Int J Pharm 324(2) (2006): 168-175.

[22] Krause, H.J., Schwarz, A., and Rohdewald, P. Polylactic acid nanoparticles, a colloidal drug delivery system for lipophilic drugs. Int J Pharm 27(2–3) (1985): 145-155.

[23] Wichert, B. and Rohdewald, P. A new method for the preparation of drug containing polylactic acid microparticles without using organic solvents. Journal of Controlled Release 14(3) (1990): 269-283.

[24] Li, F., Li, X., and Li, B. Preparation of magnetic polylactic acid microspheres and investigation of its releasing property for loading curcumin. Journal of Magnetism and Magnetic Materials 323(22) (2011): 2770-2775.

[25] Avérous, L. 9 - Synthesis, Properties, Environmental and Biomedical Applications of Polylactic Acid. in Ebnesajjad, S. (ed.)Handbook of Biopolymers and Biodegradable Plastics, pp. 171-188. Boston: William Andrew Publishing, 2013.

[26] Le Ray, A.M., et al. Vancomycin encapsulation in biodegradable poly(ε -caprolactone) microparticles for bone implantation. Influence of the formulation process on size, drug loading, in vitro release and cytocompatibility. Biomaterials 24(3) (2003): 443-449.

[27] Cao, X., et al. Core-shell type multiarm star poly(ε -caprolactone) with high molecular weight hyperbranched polyethylenimine as core: Synthesis, characterization and encapsulation properties. European Polymer Journal 44(4) (2008): 1060-1070.

[28] Payne, R.G., Yaszemski, M.J., Yasko, A.W., and Mikos, A.G. Development of an injectable, in situ crosslinkable, degradable polymeric carrier for osteogenic cell populations. Part 1. Encapsulation of marrow stromal osteoblasts in

surface crosslinked gelatin microparticles. Biomaterials 23(22) (2002): 4359-4371.

[29] Saxena, A., Sachin, K., Bohidar, H.B., and Verma, A.K. Effect of molecular weight heterogeneity on drug encapsulation efficiency of gelatin nanoparticles. Colloids and Surfaces B: Biointerfaces 45(1) (2005): 42-48.

[30] Song, X., et al. Facile fabrication of organic–inorganic composite beads by gelatin induced biomimetic mineralization for yeast alcohol dehydrogenase encapsulation. Journal of Molecular Catalysis B: Enzymatic 100(0) (2014): 49-58.

[31] Kittikaiwan, P., Powthongsook, S., Pavasant, P., and Shotipruk, A. Encapsulation of Haematococcus pluvialis using chitosan for astaxanthin stability enhancement. Carbohydrate Polymers 70(4) (2007): 378-385.

[32] Hosseini, S.F., Zandi, M., Rezaei, M., and Farahmandghavi, F. Two-step method for encapsulation of oregano essential oil in chitosan nanoparticles: Preparation, characterization and in vitro release study. Carbohydrate Polymers 95(1) (2013): 50-56.

[33] Luo, Y., Wang, T.T.Y., Teng, Z., Chen, P., Sun, J., and Wang, Q. Encapsulation of indole-3-carbinol and 3,3′-diindolylmethane in zein/carboxymethyl chitosan nanoparticles with controlled release property and improved stability. Food Chem 139(1–4) (2013): 224-230.

[34] Woranuch, S. and Yoksan, R. Eugenol-loaded chitosan nanoparticles: I. Thermal stability improvement of eugenol through encapsulation. Carbohydrate Polymers 96(2) (2013): 578-585.

[35] Koppolu, B.p., Smith, S.G., Ravindranathan, S., Jayanthi, S., Suresh Kumar, T.K., and Zaharoff, D.A. Controlling chitosan-based encapsulation for protein and vaccine delivery. Biomaterials 35(14) (2014): 4382-4389.

[36] Hearn, E. and Neufeld, R.J. Poly(methylene co-guanidine) coated alginate as an encapsulation matrix for urease. Process Biochemistry 35(10) (2000): 1253-1260.

[37] Chan, A.W. and Neufeld, R.J. Tuneable semi-synthetic network alginate for absorptive encapsulation and controlled release of protein therapeutics. Biomaterials 31(34) (2010): 9040-9047.

[38] Chan, E.-S., Yim, Z.-H., Phan, S.-H., Mansa, R.F., and Ravindra, P. Encapsulation of herbal aqueous extract through absorption with ca-alginate hydrogel beads. Food and Bioproducts Processing 88(2–3) (2010): 195-201.

[39] Chan, E.-S. Preparation of Ca-alginate beads containing high oil content: Influence of process variables on encapsulation efficiency and bead properties. Carbohydrate Polymers 84(4) (2011): 1267-1275.

[40] Shi, L.-E., et al. Encapsulation of probiotic Lactobacillus bulgaricus in alginate–milk microspheres and evaluation of the survival in simulated gastrointestinal conditions. Journal of Food Engineering 117(1) (2013): 99-104.

[41] Heitfeld, K.A., Guo, T., Yang, G., and Schaefer, D.W. Temperature responsive hydroxypropyl cellulose for encapsulation. Materials Science and Engineering: C 28(3) (2008): 374-379.

[42] Shen, J., Song, Z., Qian, X., and Yang, F. Carboxymethyl cellulose/alum modified precipitated calcium carbonate fillers: Preparation and their use in papermaking. Carbohydrate Polymers 81(3) (2010): 545-553.

[43] Panichpakdee, J. and Supaphol, P. Use of 2-hydroxypropyl- β -cyclodextrin as adjuvant for enhancing encapsulation and release characteristics of asiaticoside within and from cellulose acetate films. Carbohydrate Polymers 85(1) (2011): 251-260.

[44] Es-haghi, H., Mirabedini, S.M., Imani, M., and Farnood, R.R. Preparation and characterization of pre-silane modified ethyl cellulose-based microcapsules containing linseed oil. Colloids and Surfaces A: Physicochemical and Engineering Aspects 447(0) (2014): 71-80.

[45] Sanz-Nogués, C., Horan, J., Ryan, G., Kassem, M., and O'Brien, T. Encapsulation of human mesenchymal stem cells in sodium cellulose sulfate-based microcapsules requires immortalization. Cytotherapy 16(4, Supplement) (2014): S94.

[46] Mandal, A.S., et al. Drug delivery system based on chronobiology-A review. Journal of Controlled Release 147(3) (2010): 314-325.

[47] Li, C.L., Martini, L.G., Ford, J.L., and Roberts, M. The use of hypromellose in oral drug delivery. Journal of Pharmacy and Pharmacology 57(5) (2005): 533-546.

[48] Caraballo, I. Factors affecting drug release from hydroxypropyl methylcellulose matrix systems in the light of classical and percolation theories. Expert Opinion on Drug Delivery 7(11) (2010): 1291-1301.

[49] Liu, L., Fishman, M.L., Kost, J., and Hicks, K.B. Pectin-based systems for colon-specific drug delivery via oral route. Biomaterials 24(19) (2003): 3333-3343.

[50] Mirabedini, S.M., Dutil, I., and Farnood, R.R. Preparation and characterization of ethyl cellulose-based core–shell microcapsules containing plant oils. Colloids and Surfaces A: Physicochemical and Engineering Aspects 394 (2012): 74-84.

[51] Zheng, L., Ding, Z., Zhang, M., and Sun, J. Microencapsulation of bayberry polyphenols by ethyl cellulose: Preparation and characterization. Journal of Food Engineering 104(1) (2011): 89-95.

[52] Feczkó, T., Varga, O., Kovács, M., Vidóczy, T., and Voncina, B. Preparation and characterization of photochromic poly(methyl methacrylate) and ethyl cellulose nanocapsules containing a spirooxazine dye. Journal of Photochemistry and Photobiology A: Chemistry 222(1) (2011): 293-298.

[53] Bansode, S., Banarjee, S., Gaikwad, D., Jadhav, S., and Thorat, R. Microencapsulation: a review. International journal of pharmaceutical sciences review and research 1(2) (2010): 38-43.

[54] Liang, H.-F., et al. Novel Method Using a Temperature-Sensitive Polymer (Methylcellulose) to Thermally Gel Aqueous Alginate as a pH-Sensitive Hydrogel. Biomacromolecules 5(5) (2004): 1917-1925.

[55] Duarte, A.R., Gordillo, M.D., Cardoso, M.M., Simplicio, A.L., and Duarte, C.M. Preparation of ethyl cellulose/methyl cellulose blends by supercritical antisolvent precipitation. Int J Pharm 311(1-2) (2006): 50-4.

[56] Tunç, S. and Duman, O. Preparation of active antimicrobial methyl cellulose/carvacrol/montmorillonite nanocomposite films and investigation of carvacrol release. LWT - Food Science and Technology 44(2) (2011): 465-472.

[57] Bolzinger, M.-A., Briançon, S., Pelletier, J., and Chevalier, Y. Penetration of drugs through skin, a complex rate-controlling membrane. Current Opinion in Colloid & Interface Science 17(3) (2012): 156-165.

[58] Okajima, M.K., et al. Anionic complexes of MWCNT with supergiant cyanobacterial polyanions. Biopolymers 99(1) (2013): 1-9.

[59] Patzelt, A., et al. Selective follicular targeting by modification of the particle sizes. J Control Release 150(1) (2011): 45-8.

[60] Lademann, J., et al. Nanoparticles--an efficient carrier for drug delivery into the hair follicles. Eur J Pharm Biopharm 66(2) (2007): 159-64.

[61] Mak, W.C., et al. Triggering of drug release of particles in hair follicles. J Control Release 160(3) (2012): 509-14.

[62] Ossadnik, M., et al. Investigation of differences in follicular penetration of particle-and nonparticle-containing emulsions by laser scanning microscopy. Laser physics 16(5) (2006): 747-750.

[63] Vogt, A., et al. 40 nm, but not 750 or 1,500 nm, Nanoparticles Enter Epidermal CD1a+ Cells after Transcutaneous Application on Human Skin. Journal of investigative dermatology 126(6) (2006): 1316-1322.

[64] Subongkot, T., Wonglertnirant, N., Songprakhon, P., Rojanarata, T., Opanasopit, P., and Ngawhirunpat, T. Visualization of ultradeformable liposomes penetration pathways and their skin interaction by confocal laser scanning microscopy. Int J Pharm 441(1-2) (2013): 151-61.

[65] Rancan, F., et al. Particle-based transcutaneous administration of HIV-1 p24 protein to human skin explants and targeting of epidermal antigen presenting cells. J Control Release 176 (2014): 115-22.

[66] Chen, C.-Y., et al. Tyrosinase inhibition, free radical scavenging, antimicroorganism and anticancer proliferation activities of Sapindus mukorossi extracts. Journal of the Taiwan Institute of Chemical Engineers 41(2) (2010): 129-135.

[67] Roggero, J.-P. and Garcia-Parrilla, C. Effects of ultraviolet irradiation on resveratrol and changes in resveratrol and various of its derivatives in the skins of ripening grapes. Sciences des aliments 15(5) (1995): 411-422.

[68] Roggero, J.-P. Study of the ultraviolet irradiation of resveratrol and wine. Journal of Food Composition and Analysis 13(1) (2000): 93-97.

[69] Földes-Papp, Z., Demel, U., and Tilz, G.P. Laser scanning confocal fluorescence microscopy: an overview. International immunopharmacology 3(13-14) (2003): 1715-1729.

APPENDIX

VITA

Mr. Saranyoo Sornkamnird was born on May 31, 1990 in Uttaradit, Thailand. He obtained a Bachelor Degree of Science, majoring in Chemistry and minoring in Entrepreneurship from Chulalongkorn University and Bachelor Degree of Political Science from Ramkhamhaeng University, Bangkok, Thailand in 2011. Since 2012, he has been a graduate student studying Organic Chemistry at Department of Chemistry, Faculty of Science, Chulalongkorn University.

His present address is House No.31, Village No.6, Pa Sao sub-district, Mueang district, Uttaradit province, Thailand 53000.